science for a changing world

Geologic Map of the Southern White Ledge Peak and Matilija Quadrangles, Santa Barbara and Ventura Counties, California

Scientific Investigations Map 3321

U.S. Department of the Interior
U.S. Geological Survey

Cover *Top*, View looking west from west end of Rincon Mountain of eastern part of Santa Barbara coastal plain. *Bottom left*, View looking northeast of exposure in Devils Gulch of southeast-dipping beds of Rincon Shale (Tr) in footwall block of nearby Devils Gulch fault (not visible here; located to right of photograph view). *Bottom right*, Outcrop of gently dipping beds of conglomeratic sandstone of the Oligocene middle conglomerate and sandstone unit (Tspm) of the Sespe Formation. Lake Casitas and Laguna Ridge visible in background. Photographs by Scott A. Minor, U.S. Geological Survey.

Geologic Map of the Southern White Ledge Peak and Matilija Quadrangles, Santa Barbara and Ventura Counties, California

By Scott A. Minor and Theodore R. Brandt

Scientific Investigations Map 3321

U.S. Department of the Interior
U.S. Geological Survey

U.S. Department of the Interior
SALLY JEWELL, Secretary

U.S. Geological Survey
Suzette M. Kimball, Acting Director

U.S. Geological Survey, Reston, Virginia: 2015

For more information on the USGS—the Federal source for science about the Earth, its natural and living resources, natural hazards, and the environment—visit http://www.usgs.gov or call 1–888–ASK–USGS.

For an overview of USGS information products, including maps, imagery, and publications, visit http://www.usgs.gov/pubprod/.

Suggested citation:
Minor, S.A., and Brandt, T.R., 2015, Geologic map of the southern White Ledge Peak and Matilija quadrangles, Santa Barbara and Ventura Counties, California: U.S. Geological Survey Scientific Investigations Map 3321, 34 p., 1 sheet, 1:24,000, http://dx.doi.org/10.3133/sim3321.

ISSN 2329-132X (online)

Contents

Sheet

Figures

Conversion Factors

Multiply	By	To obtain
millimeter (mm)	0.03937	inch (in.)
centimeter (cm)	0.3937	inch (in.)
meter (m)	3.281	foot (ft)
kilometer (km)	0.6214	mile (mi)

Geologic Map of the Southern White Ledge Peak and Matilija Quadrangles, Santa Barbara and Ventura Counties, California

By Scott A. Minor and Theodore R. Brandt

Introduction

This report presents a digital geologic strip map of the southern parts of the contiguous White Ledge Peak and Matilija 7½′ quadrangles in coastal southern California at a compilation scale of 1:24,000 (map plate; figs. 1 and 2). The map depicts the distribution of bedrock units and surficial deposits and associated deformation adjacent to and south of the Arroyo Parida fault (including faults on trend with it east of the Ventura River) (fig. 3). The overall objective of the new mapping presented herein is to extend recent geologic mapping of the Santa Barbara coastal plain by the U.S. Geological Survey (USGS) (Minor and others, 2009) as far east as Sulphur Mountain and Ojai Valley (figs. 2 and 3).

This geologic map, combined with the recently published adjacent map to the west (Minor and others, 2009), completes a 69-kilometer (km)-long east-west transect between the cities of Goleta and Ojai (fig. 2). These geologic transect maps and the associated sedimentologic, biostratigraphic, stratigraphic, and structural data embedded within them, provide new insights to and constraints on Neogene-through-Quaternary tectonic deformation, uplift, syntectonic sedimentation, and consequent landscape change as well as geohazards in the urbanized coastal hills, plains, and valleys along the southern flank of the Santa Ynez Mountains. The present compilation builds on the earlier foundation geologic mapping by Thomas Dibblee, Jr. (Dibblee, 1987a,b) and presents new detailed map data that refine geologic knowledge and interpretations along a key segment of the regional map transect where the Arroyo Parida and similar striking faults approach and interact with the tip regions of the potentially seismogenic Red Mountain and San Cayetano faults located to the southeast and east, respectively, of the map area (fig. 2) (Yeats, Lee, and Yerkes, 1987; Rockwell, 1988; Huftile and Yeats, 1995). The principal aim of the new mapping and associated fault-kinematic measurements (see below) is to document and constrain the nature of transpressional strain transfer between these various faults.

The map area, located in the western Transverse Ranges (WTR) physiographic province, forms a 22-km-long strip that extends eastward (inland) from Carpinteria at the east end of the Santa Barbara coastal plain to Ojai (figs. 1, 2, 3, and 4). The Santa Ynez Mountains and large coastal hills border it on the north (figs. 2 and 3) and south, respectively. The Santa Ynez Mountains, the most prominent mountain block of the coastal WTR, extend for more than 100 km and rise abruptly as much as 1,225 meters (m) (4,000 feet [ft]) above the adjacent coastal alluvial plains, valleys, and hills.

The coastal terrain bordering the Santa Ynez Mountains, along with the adjacent Santa Barbara Channel, coincide with a zone of moderate seismicity that poses some risk to people living in the densely populated Santa Barbara-Ojai-Ventura metropolitan corridor. A major (~7 magnitude (M)) earthquake occurred in the Santa Barbara Channel in 1812, and other strong earthquakes have occurred offshore within 10 km of the Santa Barbara coastal plain in 1925 (M6.3), 1941 (M5.5), and 1978 (M5.1) (for example, Yerkes and others, 1981; Yerkes and Lee, 1987). Numerous Quaternary landslide deposits along the steep slopes of the Santa Ynez Mountains (Bezore and Wills, 2000; Tan and Clahan, 2004; Tan and Jones, 2006) and adjacent coastal uplands indicate the potential for continued slope failures in developed areas.

Folded, faulted, and fractured sedimentary rocks in the subsurface of the coastal plains and hills within and south of the map area, including the adjacent Santa Barbara Channel, are sources and reservoirs for economic deposits of oil and gas (Tennyson and Isaacs, 2001), some of which are currently being extracted offshore. Shallow, localized, sedimentary aquifers underlying the Santa Barbara coastal plain and Ojai Valley-Ventura River area provide limited amounts of water for nearby urban areas (Upson, 1951; Muir, 1968; Kear, 2005).

The present map compilation provides a set of uniform geologic digital geodatabase and shape files that can be used for analysis and interpretation of these and other geologic hazards and resources in the map area.

The digital geodatabase for this map and a map plot file (PDF) are available on the Internet at: http://dx.doi.org/10.3133/sim3321.

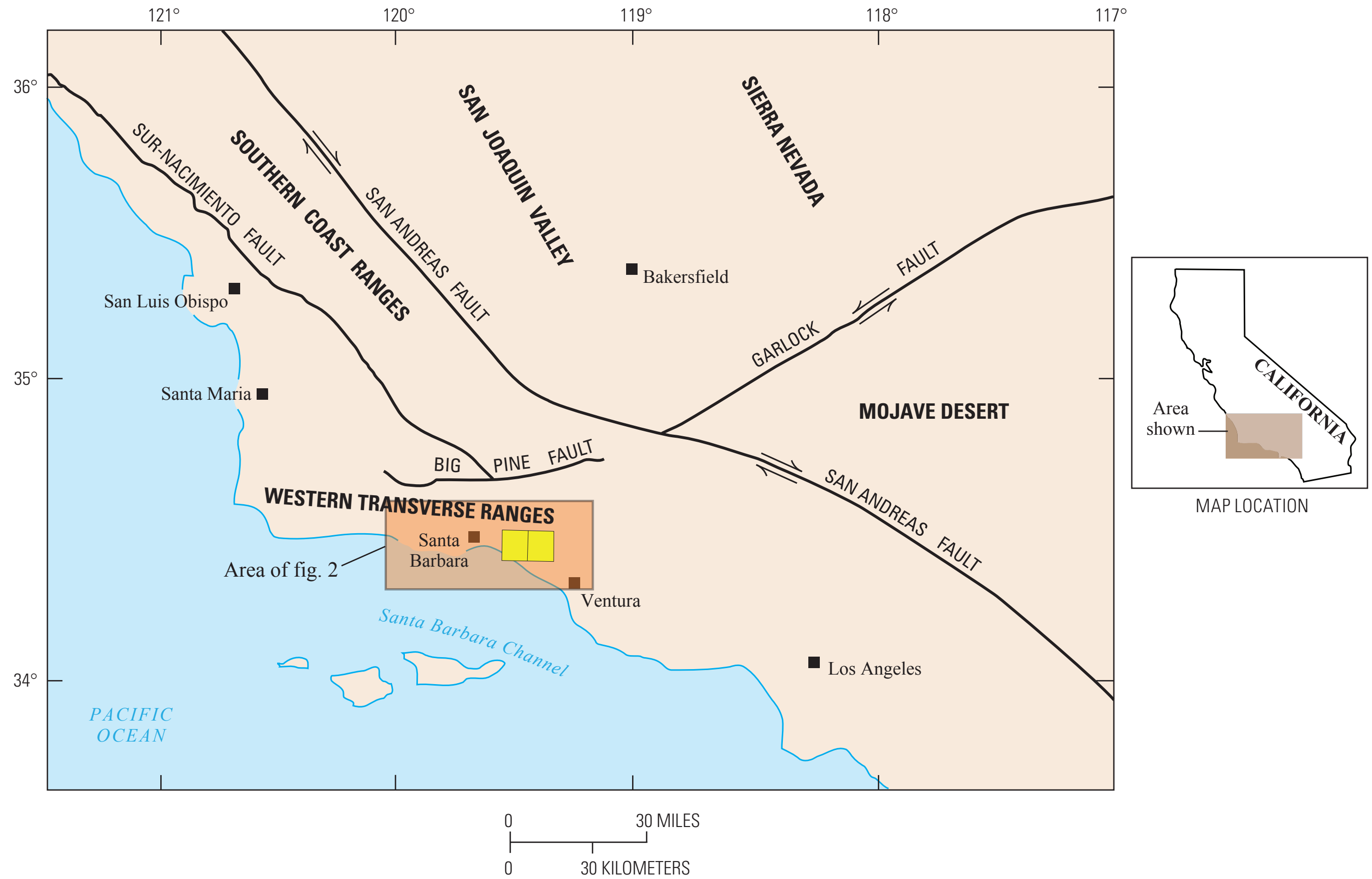

Figure 1. Generalized location map of part of southwestern California showing major tectonic faults, the area of fig. 2 (in orange), and the two quadrangles containing the geologic mapped area (in yellow).

Previous Mapping

The earliest systematic geologic mapping in the map area was by Upson (1951), who mapped the Santa Barbara coastal plain region in reconnaissance at a scale of 1:31,680 as part of a water-resource study, and by Lian (1954), who mapped the eastern part of the coastal plain area at a scale of 1:62,500. As part of their thesis-dissertation research Clark (1982) and Rockwell (1983) mapped the geology of the Ojai Valley and upper Ventura River area at a scale of 1:24,000, with Rockwell's mapping focused on the distribution and age of elevated late Pleistocene fluvial terraces. The Thomas Dibblee Foundation published geologic maps of the White Ledge Peak and Matilija 7½' quadrangles at a scale of 1:24,000 (Dibblee, 1987a,b).

More recent "preliminary" geologic maps of these two quadrangles by the California Geological Survey (formerly California Division of Mines and Geology) (Tan and Clahan, 2004; Tan and Jones, 2006) largely reproduce the Dibblee bedrock mapping but include extensive new mapping of landslide deposits and related features. The California Geological Survey also produced 1:24,000 scale landslide inventory and landslide potential maps of the Santa Barbara coastal plain region, which include the present map area west of Rincon Creek (Bezore and Wills, 2000).

New Mapping

Field-based geologic mapping and associated fault-kinematic investigations in the map area were conducted by S.A. Minor chiefly in 2007 through 2011. T.R. Brandt assisted in the design and editing of the geographic information system (GIS) data that are used in the digital geodatabase and performed database integration. The present geologic map is based on new mapping from observations and interpretations made at the ground surface or in shallow surface excavations, analysis of aerial photographs (map plate), and new biostratigraphic data. Owing mainly to the questionable or conflicting stratigraphic picks in many of the drilling logs in the map area, no geologic cross sections are presented herein. The recently revised geologic time scale of the U.S. Geological Survey Geologic Names Committee (2010) was adopted for assigning geologic ages to the Tertiary map units in this report, whereas the chronostratigraphic chart of Cohen and others (2013) was used to assign ages to the subdivisions of the Quaternary. In the description of map units, sedimentary lithologic terms and rock naming conventions are largely from Williams and others (1982).

The new mapping of the White Ledge Peak and Matilija quadrangles broadly resembles the earlier Dibblee (1987a,b) mapping that has served as the principal geologic map reference in the area, but it differs significantly in the amount of

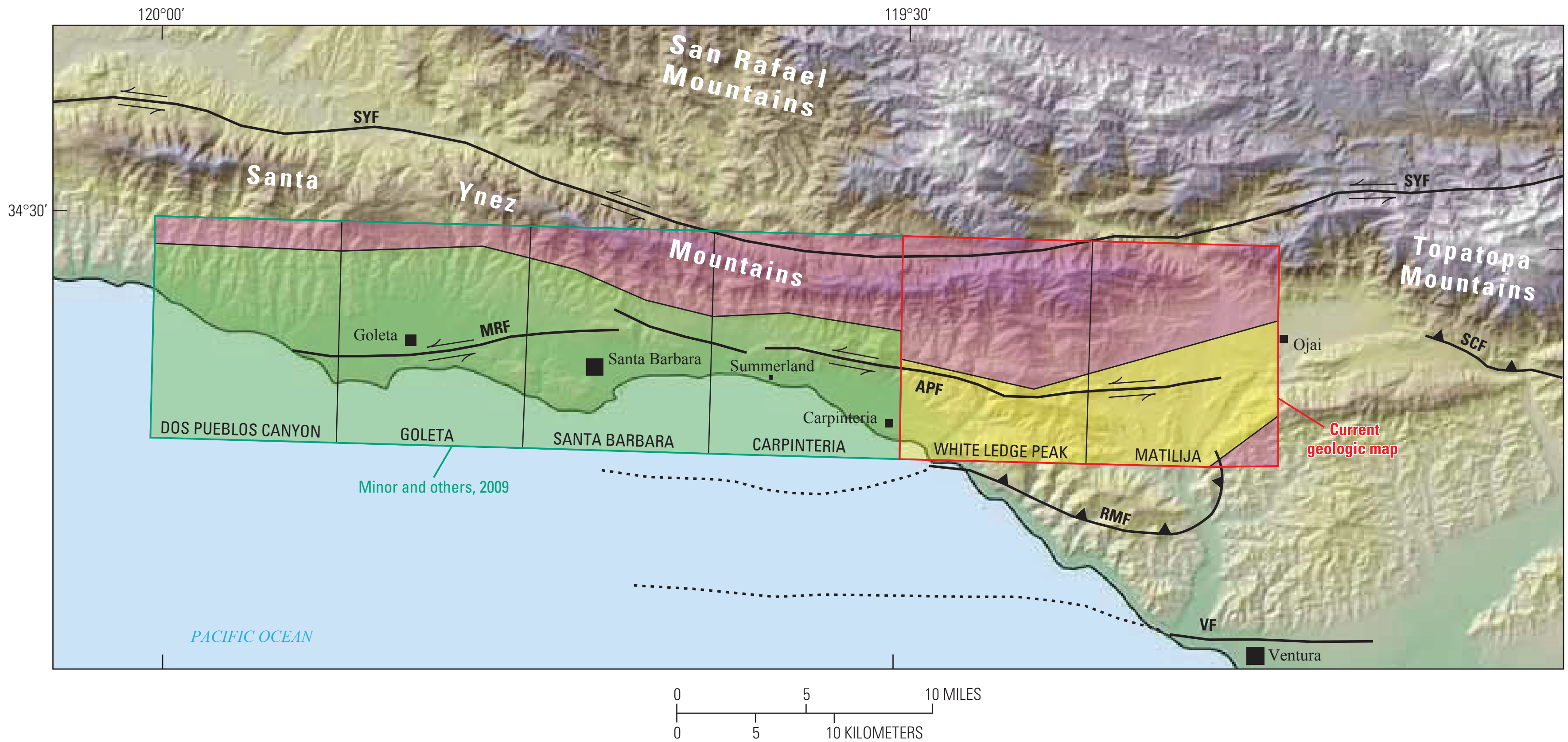

Figure 2. Regional physiographic map showing location of the current map area (yellow shading), previously published geologic map of the Santa Barbara coastal plain area; (Minor and others, 2009; green shading), 7½′ topographic quadrangles overlapping geologic map areas (pink shading), and major tectonic faults (thick black lines). Faults: SYF, Santa Ynez; SCF, San Cayetano; RMF, Red Mountain; VF, Ventura; APF, Arroyo Parida; MRF, More Ranch. Fault symbols: barbs, thrust fault (barbs on upper plate); paired opposing arrows, sense of strike-slip movement, dotted lines where concealed. The base map is derived from the U.S. Geological Survey National Elevation Dataset (NED), 10-meter resolution elevation data, 2005; hillshading illuminated from the northwest; color ramping based on relative elevation, with dark green corresponding to lowest elevations and white indicating highest elevations.

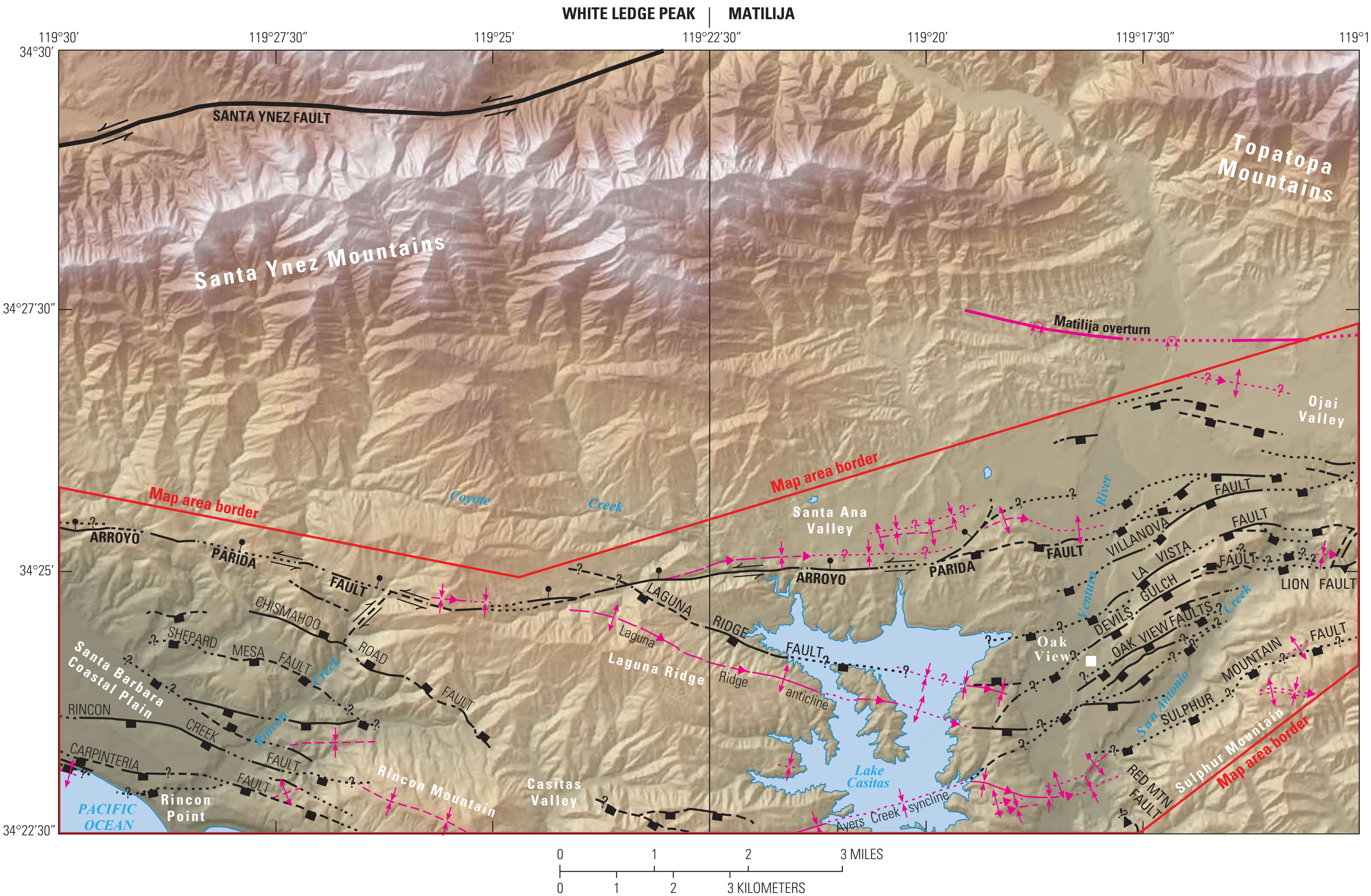

Figure 3. Tectonic and physiographic map of the combined White Ledge Peak and Matilija quadrangles showing faults (black lines) and folds (magenta lines) mapped in this study and other major structural features in the vicinity (thick black and magenta lines). Location of town is labeled and marked with white square. The geologic map area is outlined in red. Structural lines and symbols are the same as those used on geologic map. The digital elevation model (DEM), hypsometric tint, and shaded-relief values composing the base map are derived from the U.S. Geological Survey National Elevation Dataset (NED), 10-meter resolution elevation data, 2005.

EXPLANATION

Fault—Queried where uncertain; ball on downthrown side indicating older normal slip; opposing arrows indicate sense of younger strike-slip component of movement

Thrust fault—Queried where uncertain, dashed where location approximate; sawteeth on upthrown side

Reverse fault—Queried where uncertain, dashed where location approximate, short dash where inferred, dotted where concealed; exhibits reverse component of slip; boxes on upthrown side

Anticline—Queried where uncertain, dashed where location approximate, short dash where inferred, dotted where concealed; large arrowhead shows direction of plunge

Syncline—Queried where uncertain, dashed where location approximate, short dash where inferred, dotted where concealed; large arrowhead shows direction of plunge

Syncline, overturned—Queried where uncertain, dashed where location approximate, short dash where inferred, dotted where concealed; large arrowhead shows direction of plunge

Figure 3.—Continued.

stratigraphic and, especially, structural detail and in the resulting geologic interpretations and map depictions. The present compilation includes detailed description, differentiation, and mapping of Pleistocene marine and nonmarine units that bear on the Quaternary tectonic uplift and deformational history of the map region and the attendant interplay of marine and continental deposition. Structures are mapped in considerably greater detail than on the previously published maps, resulting in a more thorough and, in places, distinct documentation of faults and folds in Quaternary deposits.

Fault-Kinematic Measurements

As part of efforts to document the structural geology and tectonic evolution of the map area, 132 kinematic data (slip-surface orientation and slickenline rake measurements and slip-sense determinations) were collected from 73 smaller-displacement (<5 m) “mesoscale” fault surfaces and 19 larger-displacement (5 to >100 m) fault surfaces exposed in the map area within sedimentary rocks and deposits ranging in age from middle Eocene (Coldwater Sandstone, unit Tcw) to late Pleistocene (intermediate alluvial deposits, unit Qia, and marine-terrace deposits, unit Qmt) (fig. 5*A*,*B*). Slip lineation (mostly striation) bearing and rake measurements taken at exposures of larger-displacement faults are shown in red on the cartographic representation of the map, whereas all of the kinematic data (slip-lineation bearing, rake, slip sense, slip-sense certainty) from both the larger- and smaller-displacement faults are embedded as “point” data in the geodatabase. The slip sense of faults that do not offset beds or other distinctive stratigraphic or structural features was determined or inferred using secondary fractures, mineral coatings, or other shear-sense indicators preserved on the principal slip surfaces (fig. 6) (Petit, 1987; Doblas, 1998).

Also recorded were relative-age observations of faults and fault slip, especially crosscutting relations of multiple sets of slickenlines on reactivated faults. These fault-kinematic data may provide important constraints for the timing and rates of uplift and movement histories of fault blocks, which may also reveal significant tectonic controls on the geomorphic evolution of Neogene to recent landscapes of the region. The fault-kinematic data will also likely provide constraints for future regional seismic hazards models.

Geologic Summary

The western Transverse Ranges consist mainly of variably deformed marine and nonmarine sedimentary rocks and deposits that range in age from Jurassic to Holocene. These strata record a long history of continental-margin sedimentation, and deposits as young as late Pleistocene record considerable protracted deformation that includes Neogene and Quaternary transpressional faulting, folding, and clockwise vertical-axis rotations of crustal blocks (for example, Dibblee, 1966, 1982; Hornafius and others, 1986; Namson and Davis, 1988; Luyendyk, 1991; Dickinson, 1995; Gurrola and others, 2014). A dramatic result of this deformation is the prominent Santa Ynez Mountains lying directly north of the map area (fig. 3), which were uplifted along a large homoclinal-to-anticlinal structure beginning in the Pliocene (Dibblee, 1982).

In the map area, the oldest stratigraphic units are Eocene and consist of resistant, southward-dipping, mostly marine sedimentary rocks that are only locally exposed. Just north of the map area, however, these rocks form a backdrop of prominent hogbacks and cuestas along the south flank of the Santa Ynez Mountains uplift (fig. 3). Less resistant but similarly-dipping and folded Oligocene through Pliocene terrestrial and marine sedimentary rocks make up most of the coastal hills and sea

Figure 4. View looking west from west end of Rincon Mountain of eastern part of Santa Barbara coastal plain. City of Carpinteria and Rincon Point are visible in right and left center of photograph, respectively. Part of extensive landslide complex on south flank of Rincon Mountain is visible in lower left part of photograph (area of bright green vegetation). Southwest part of map area includes landscape visible in lower half of photograph.

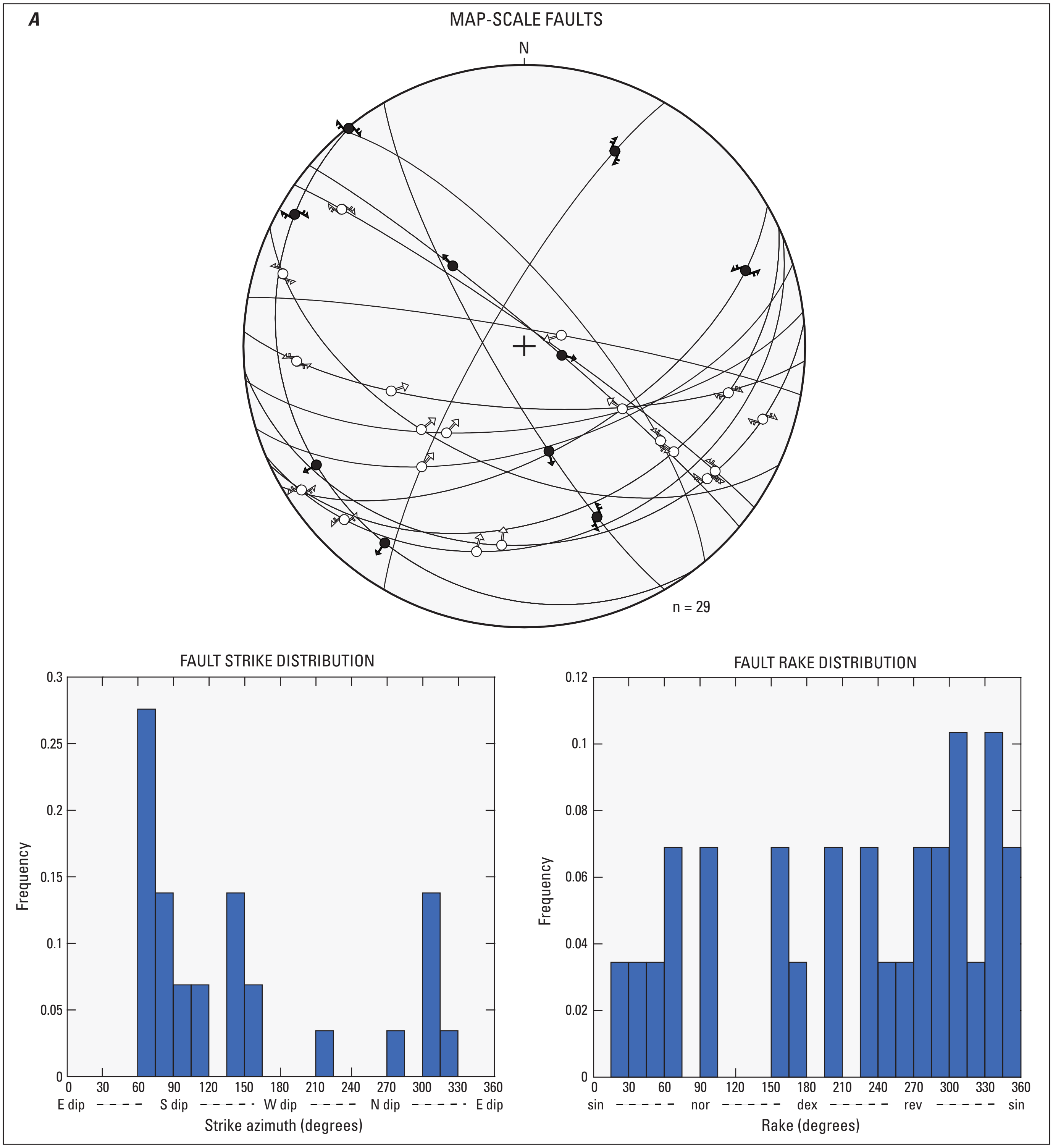

Figure 5. Structural plots of slip observations of *A*, Map-scale (plotted on map) and *B*, Mesoscale faults (see database for measurements and coordinates) exposed in map area. Upper circular plots are lower-hemisphere, equal-area projections of fault slip surfaces (great circles) and slickenlines (points); small arrows attached to points indicate slip sense (strike-slip-dominant faults) or hanging-wall movement direction (dip-slip-dominant faults); reverse and normal slip components indicated by open and filled points/arrows, respectively; N, north; n, number of fault-slip measurements. Lower histograms show fault strike and rake frequency distributions; frequency axis values are scaled to decimal fractions of the total number of measurements; strike azimuths are 90° counterclockwise from fault dip directions; rake values range from 0° to 360°, where 0° (=360°) is pure sinistral (sin) strike slip, 90° is pure normal (nor) slip, 180° is pure dextral (dex) strike slip, and 270° is pure reverse (rev) slip.

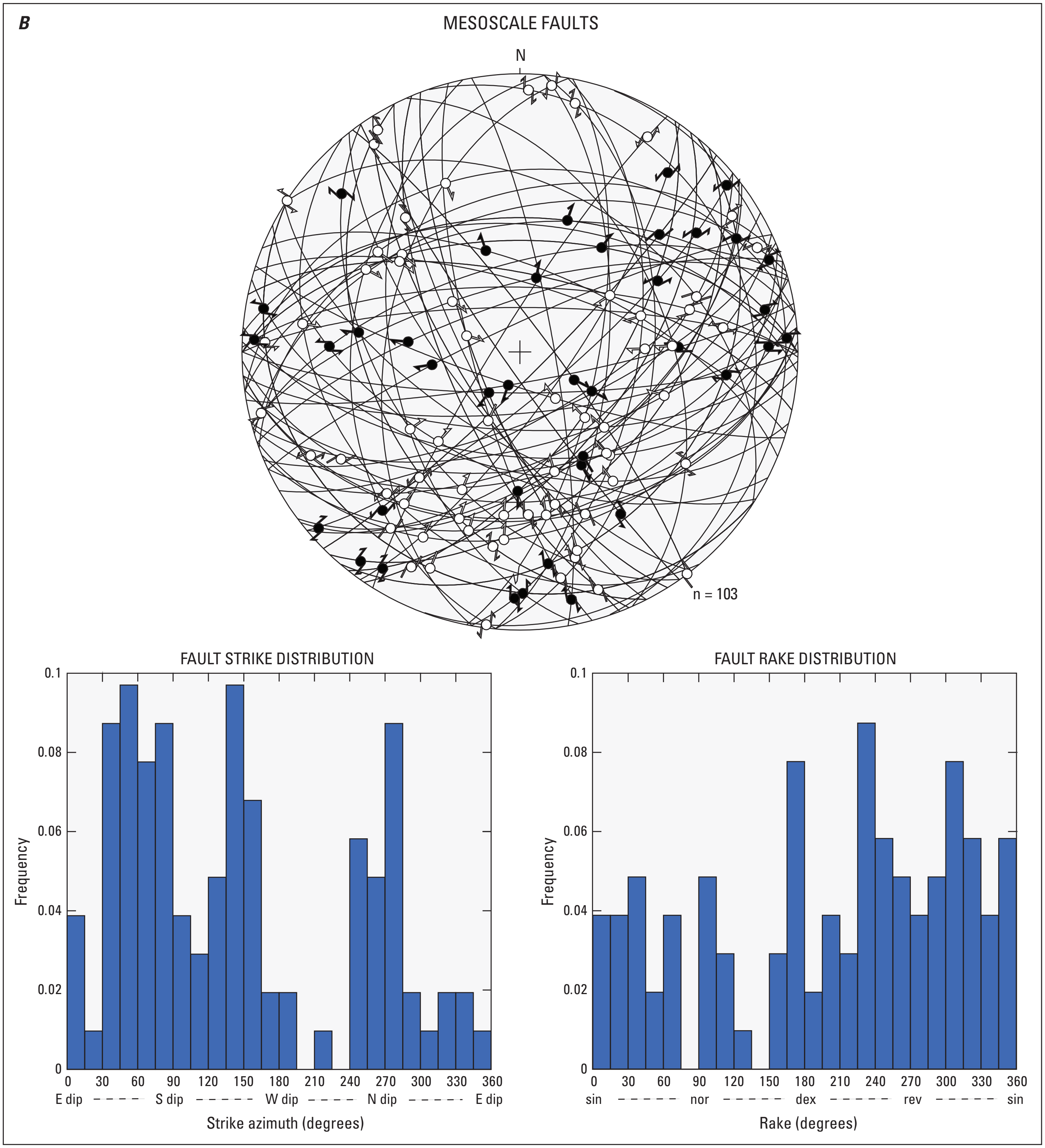

Figure 5. Structural plots of slip observations of *A*, Map-scale (plotted on map) and *B*, Mesoscale faults (see database for measurements and coordinates) exposed in map area. Upper circular plots are lower-hemisphere, equal-area projections of fault slip surfaces (great circles) and slickenlines (points); small arrows attached to points indicate slip sense (strike-slip-dominant faults) or hanging-wall movement direction (dip-slip-dominant faults); reverse and normal slip components indicated by open and filled points/arrows, respectively; N, north; n, number of fault-slip measurements. Lower histograms show fault strike and rake frequency distributions; frequency axis values are scaled to decimal fractions of the total number of measurements; strike azimuths are 90° counterclockwise from fault dip directions; rake values range from 0° to 360°, where 0° (=360°) is pure sinistral (sin) strike slip, 90° is pure normal (nor) slip, 180° is pure dextral (dex) strike slip, and 270° is pure reverse (rev) slip.—Continued

Figure 6. Close-up photograph of principal fault slip surface, formed in pebbly sandstone bed of the Rincon Shale (Tr), preserving carbonate mineral coatings (white patches) that were precipitated in the fault zone during its slip history. Slickenside striae (trending diagonally across photograph from upper right to lower left), along with distribution of mineral coatings preferentially on lower left sides of surface asperities, indicate that missing fault block slipped in direction of black arrow. Coin is about 2.5 cm in diameter.

Figure 7. Outcrop of gently dipping beds of conglomeratic sandstone of the Oligocene middle conglomerate and sandstone unit (Tspm) of the Sespe Formation. Lake Casitas and Laguna Ridge visible in background.

cliffs in the map area (figs. 7, 8, and 9). Less tilted, but moderately faulted, Pleistocene marine and terrestrial sediments underlie many of the smaller hills and mesas bordering the east end of the Santa Barbara coastal plain and in the Oak View-Ojai Valley area (figs. 3, 10, and 11). Undisturbed Holocene alluvial deposits underlie the floodplains of the Ventura River and larger stream valleys and Quaternary landslides and landslide complexes are common on steeper mountain flanks, particularly on Rincon Mountain and Sulphur Mountain (figs. 3 and 12).

Structural and Kinematic Framework

Structurally, the map area is dominated by an array of subparallel faults and lesser folds that is continuous with the Santa Barbara fold and fault belt transecting the Santa Barbara coastal plain area directly to the west (Minor and others, 2009; Gurrola and others, 2014) (fig. 3). In the map area this structural belt is roughly arcuate in plan, containing structures that change in trend from west-northwest in the western part of the map area to east-northeast in the eastern part (map plate and fig. 3).

In the map area, the fault and fold belt is bounded on the north by the large-trace-length (30 km total; 20 km in map area) Arroyo Parida fault, which, near Pike Spring (western part of map area), abruptly changes ~20° in strike from west-northwest (west of bend) to east-northeast (east of bend). The Arroyo Parida fault continues to the east of this bend for about 8 km mostly as a single trace before it splays and eventually merges with other, smaller subparallel faults where it approaches and crosses the Ventura River. The Arroyo Parida can no longer be confidently traced as a single, distinct fault east of the river valley.

The Arroyo Parida fault has had a complex movement history in the Neogene and Quaternary involving significant, early (late Miocene?) normal(?) dip slip as well as later (Plio-Pleistocene) strike slip and reverse-oblique slip (Minor and others, 2009). Early normal movement on the Arroyo Parida is inferred from (1) its apparent north dip based on its trace over irregular topography in the western part of the map area, (2) common juxtaposition of stratigraphically older rock units on the south side of the fault, and (3) kinematic evidence of early normal slip on similarly oriented faults in the Santa Barbara coastal plain area west of the map area (Minor and others, 2009). Near-fault sinistral deflections (drag?) of bedding in bedrock (Eocene and Oligocene Sespe Formation, units Tspl, Tspm, and Tspu) suggest that sinistral strike slip accompanied or followed the normal slip. The Arroyo Parida fault likely accommodated a large component of sinistral strike slip in the Quaternary based on sinistral deflections of several stream channels that cross the fault trace in the map area (for example, Coyote Creek near its confluence with Lake Casitas) and north of Carpinteria and Summerland, 10 km west of the map area (figs. 2 and 3) (Dibblee, 1966; Gurrola and others, 2001; Minor and others, 2009). Vertically displaced late Pleistocene alluvial terraces (Qia4 and Qia3) on either side of the Ventura River suggest an additional component of youthful south-side-up dip slip along at least the easternmost part of the Arroyo Parida. Although direct kinematic characterization of the Arroyo Parida is precluded in the map area due to the lack of exposures of its principal slip surface, the prevalence of similar-striking reverse faults observed elsewhere in the area (see discussion below) suggest that the late Neogene and younger dip-slip components of movement may have been reverse along the Arroyo Parida.

Figure 8. View looking northeast of exposure in Devils Gulch of southeast-dipping beds of Rincon Shale (Tr) in footwall block of nearby Devils Gulch fault (not visible here; located to right of photograph view). Flat surface covered with grass and shrubs above gulch on left side is late Pleistocene intermediate alluvial strath terrace (Qia4) that is also cut by Devils Gulch and other subparallel faults.

Figure 9. View looking northeast along hinge of anticline formed in shale and mudstone of the upper siliceous unit of the Monterey Formation (Tmu). Fold is exposed in Highway 33 roadcut in southeastern part of map area about 1.5 km north of its southern border. Pick in lower center of photograph is about 0.5 m in length.

Figure 10. Lion Creek cutbank exposure (near central east border of map area) of moderately dipping boulder-, cobble-, and pebble-bearing conglomerate of Ojai (Qco) which here unconformably overlies Rincon Shale (Tr) with minor angular discordance. Clasts in the middle(?) Pleistocene conglomerate of Ojai are mostly derived from the Eocene and Oligocene sedimentary units exposed along the south flank of the nearby Santa Ynez Mountains uplift.

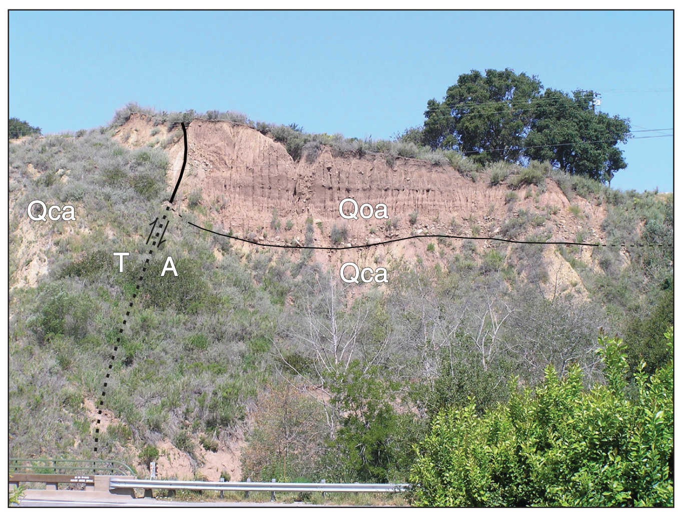

Figure 11. View looking west of Rincon Creek cutbank exposure of Rincon Creek fault, here juxtaposing tilted Pleistocene strata of the Casitas Formation (Qca) in the upthrown (left) block against horizontally bedded upper(?) Pleistocene older alluvial deposits (Qoa) and unconformably underlying Casitas deposits (Qca). Fault principal slip surface excavated near top of exposure reveals reverse-sinistral oblique-slip kinematic indicators. Dotted line indicates the location is concealed. A, fault movement away from observer, T, toward the observer.

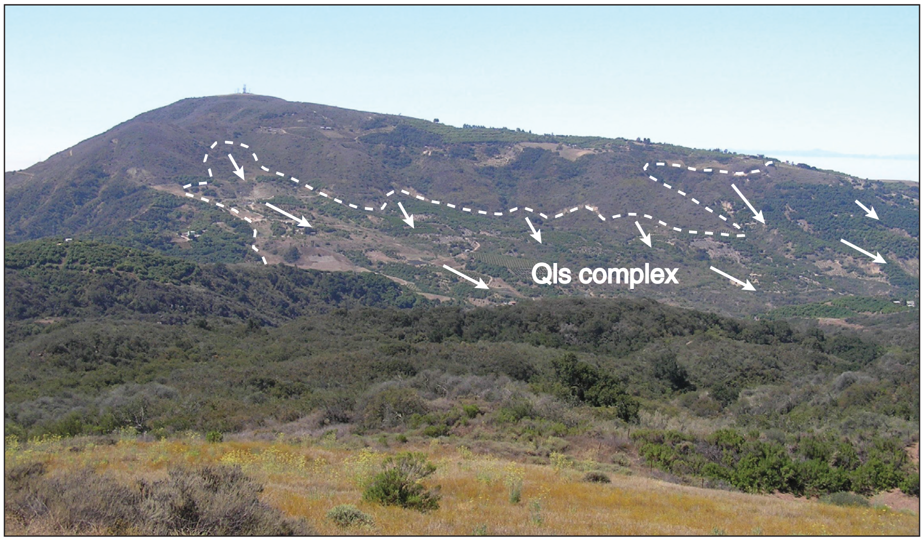

Figure 12. View looking south of landslide (Qls) complex on north flank of Rincon Mountain. Landslide deposits, which have slid and flowed downslope in directions indicated by arrows, were sourced in mudrocks of the Rincon Shale (Tr) and lower calcareous unit of the Monterey Formation (Tml) that underlie upper slopes of Rincon Mountain. White dashed line delineates the approximate location of the composite headwall scarp of the slumped area.

Most map-scale faults defining the structural grain of the fault and fold belt in the map area are either inferred or directly observed to be reverse and oblique reverse in nature. Inferences of reverse faulting are based on one or a combination of several of the following observations: (1) the presence of stratigraphically older rocks or deposits in the hanging-wall block where the fault dip direction can be determined (fig. 13); (2) alluvial terrace cut by the fault is more elevated on the hanging-wall block; (3) abrupt steepening, overturning, or asymmetrical folding of beds on one or both sides of the fault, verging towards the down-dropped block. Reverse and oblique-reverse slip is confirmed by direct kinematic observations on exposed principal slip surfaces of mapped faults (fig. 5*A*). More than half (59 percent) of the slip lineation rake angles measured on the fault surfaces lie within the reverse–oblique-reverse range (195°–345°).

A majority of the measured mesoscale faults similarly have reverse components of slip, although these smaller faults have a much broader strike range (fig. 5*B*). Most of the directly measured fault surfaces dip moderately to shallowly to the south and south-southwest. Presumably the same is true for most of the inferred reverse faults, which are similarly upthrown on their southern sides. One prominent exception is the Chismahoo Road reverse fault in the western part of the map area, whose curving trace across rugged topography and overturned southern (downthrown) block imply a north-northeasterly dip. Kinematic observations indicate that some faults have experienced dominantly strike-slip movement (fig. 5*A*,*B*), in some cases either pre- or post-dating reverse movement on the same slip surface. No clear, consistent correlation of strike slip sense (that is, sinistral or dextral) with fault strike has been identified in the map area.

Strata in the map area predominantly dip gently to moderately (10°–55°) to the south, the main exceptions being in the areally restricted north-dipping limbs and plunging noses of folds (figs. 8 and 9). This stratal tilt pattern is consistent with and likely genetically related to the regionally extensive south-dipping flank of the Santa Ynez Mountains uplift present north and northwest of the map area, which is grossly homoclinal but in detail characterized by domains of overturned strata with steep to moderate dips (Dibblee,

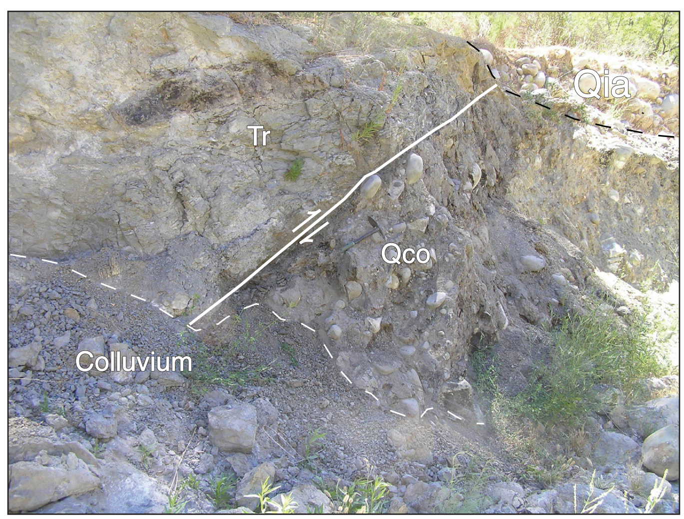

Figure 13. View looking west of Lion thrust fault exposed in cut bank of Lion Creek. Here fault thrusts Miocene Rincon Shale (Tr) over tar-impregnated Pleistocene conglomerate of Ojai (Qco). Late Pleistocene alluvial terrace (Qia) overlies and postdates fault. Pick in center of photograph is about 0.5 m in length. Dashed line indicates contact location is approximate.

1966, 1982; Minor and others, 2009). A panel of moderately to steeply overturned, north-dipping Tertiary strata on either side of Rincon Creek (western part of the map area, fig. 3) forms the footwall block of the Chismahoo Road fault, with the vergence of the overturned strata consistent with southward displacement of the upthrown (hanging-wall) block of the fault.

Most folds are located in the eastern part of the map area, where they range in trend from west-northwest to east-northeast, subparallel to nearby fault traces, and generally plunge gently (<10°) to moderately (10°–30°) eastward (figs. 3, 9). Two prominent folds with long (5–8 km) axial traces project across Lake Casitas, the Ayers Creek syncline and Laguna Ridge anticline (fig. 3). The north-vergent Laguna Ridge fold is a hanging-wall anticline probably associated with reverse slip on the adjacent Laguna Ridge fault to the north, and the fold seems to merge with a separate up-to-south reverse fault where it projects eastward into the low hills east of Lake Casitas (fig. 3). In contrast, the symmetric Ayers Creek syncline is not clearly related to slip on any adjacent, co-extensive fault exposed at the surface, but the north fold limb is cut by a reverse fault that merges westward with the fold's axial trace where it crosses the east shore of Lake Casitas. Several smaller folds are present on the north side of, and trend subparallel to, the trace of the Arroyo Parida fault in the Santa Ana Valley area in the northeast part of the map area (fig. 3). Two notable folds are located in the western part of the map area: (1) a northwest-trending syncline whose axial trace is in rocks of the Monterey Formation (Tml) underlying the western ridge crest of Rincon Mountain (fig. 3), and (2) a west-trending and -plunging syncline formed in deposits of the Casitas Formation (Qca).

A series of reverse and oblique-reverse faults cutting Oligocene and Miocene sedimentary bedrock (units Tspu, Tv, Tr, Tml, and Tmu) and Pleistocene alluvial terrace deposits (units Qia6, Qia5, Qia4, Qia3, and Qia2) in the Ventura River-Oak View area (eastern part of map area, fig. 3) strike northeast and dip southeast, subparallel to bedding attitudes in the area (figs. 8, 13, and 14). These up-to-south reverse faults have been interpreted to have formed by flexural slip of underlying Tertiary strata accommodating late Neogene and Quaternary folding in the area, including development of the Ayers Creek syncline (Clark, 1982; Rockwell, 1983; Rockwell and others, 1984). Alternatively, or additionally, oblique-reverse faulting in this area may accommodate the eastward termination or transfer of sinistral slip on the Arroyo Parida fault.

Most faults in the map area cut Quaternary marine (Qsb and Qmt) and terrestrial (Qca, Qco, Qoa, and Qia6 to Qia2) deposits as young as late Pleistocene, similar to that documented in the fault and fold belt to the west (Minor and others, 2009; Gurrola and others, 2014), indicating that much of the deformation is youthful. Such young deformation is perhaps best expressed geomorphically by the faulted Pleistocene deposits and alluvial terraces in the Oak View-San Antonio Creek areas (fig. 3), where reverse faults form a series of fault scarps where they vertically displace a sequence of late Pleistocene alluvial terraces (figs. 13 and 14). In the Carpinteria area at the east end of the Santa Barbara coastal plain (southwesternmost part of map area, fig. 3), the Carpinteria and Rincon Creek faults are also geomorphically well-expressed by locally prominent, north-facing, fault-fold scarps and broad anticlinal upwarps formed in middle and late Pleistocene deposits (Qca, Qoa, and Qmt) on their southern, upthrown blocks (fig.11).

Furthermore, the late Pleistocene sequence of marine terraces (Qmt) in this area gradually (but steadily) rises in elevation eastward from Carpinteria and lower Rincon Creek to the southern border of the map area and farther southeast towards Ventura, providing direct evidence of dramatic post 45 ka (kilo-annum, thousand years) tectonic uplift in the region (Yerkes and Lee, 1987). The occurrence of earlier (pre-Quaternary?) stratal tilting in the map area, and possibly related folding and faulting, are indicated by small to moderate (<20° to >50°) angular unconformities that separate Tertiary sedimentary bedrock units from overlying early(?) and (or) middle(?) Pleistocene deposits (Qsb, Qca, and Qco) (fig. 10).

Figure 14. Panorama looking west-to-southwest across San Antonio Creek valley, of a faulted late Pleistocene alluvial strath terrace (Qia6). Terrace, expressed as gently south-tilted "treads" visible along ridge crest in upper center and left parts of photograph, is cut by a series of intervening southwest-striking, south-side-up oblique-reverse faults expressed as north-facing slopes or "risers" visible in upper left, center, and right parts of photograph. Lower bench visible on far-right side of photograph and open grassy surface in center foreground are younger alluvial terraces (Qia3 and Qia2, respectively) that postdate faulting.

DESCRIPTION OF MAP UNITS

[Unit symbols are queried on map where the unit identification is questionable. The database contains additional features (minor folds and faults) that do not appear on the map]

SURFICIAL DEPOSITS

MAN-MADE DEPOSITS

af **Artificial fill (Holocene)—**Mappable areas of fill used for construction of highways, roads, buildings, and dams. Thickness mostly less than 10 m, but locally exceeds 30 m

ALLUVIAL DEPOSITS

Qa **Active alluvium (Holocene)—**Unconsolidated sediments, primarily pebble to boulder gravel, in floors and banks of modern stream and river channels and floodplains. Sediments subject to seasonal flooding and downstream transport. Active channels incised as much as 5 m into older alluvial deposits (for example, Qya). Includes active alluvium of Ventura River in east part of map area. Thickness of unit generally less than 5 m

Qya **Younger alluvium (Holocene)—**Unconsolidated to weakly consolidated, poorly to moderately sorted silt, sand, and pebble to boulder gravel occupying the broad valley floors and floodplains of larger drainages. Unit typically forms extensive, non-dissected terraces that flank, and lie less than 3 m above, active stream and river channels and their associated alluvium (Qa). Younger alluvium present mainly along the Ventura River and within the San Antonio, Rincon, and Carpinteria Creek drainages, where it is rarely subject to flooding. Adjacent to valley and canyon margins unit locally includes subordinate colluvial deposits containing poorly sorted, angular clasts. Terrace surfaces formed by alluvium commonly contain poorly to moderately developed soil profiles and are sparsely to moderately vegetated with grasses, shrubs, and trees. Younger alluvium previously mapped as stream gravel and “abandoned meanders of San Antonio Creek” (Clark, 1982); modern river gravels and Oak View floodplain and terraces “Q1”, “Q2”, and “Qt3” (Rockwell, 1983); alluvium (Dibblee, 1987a,b); alluvial deposits (Tan and Clahan, 2004); and alluvial and colluvial deposits (Tan and Jones, 2006). Younger alluvium deposits estimated to range in age from <250 years before present (yr B.P.) to about 5 kyr (thousand years) B.P. (Rockwell, 1983; Rockwell and others, 1984). Thickness of younger alluvium generally less than about 4 m

Qaf **Alluvial fan deposits (Holocene and late Pleistocene?)—**Weakly to moderately consolidated, poorly to moderately sorted silt, sand, and pebble to boulder gravel forming weakly to moderately dissected fans. Deposits form a broad fan-like apron in the town of Ojai, small fans along Rincon Creek, and a fan delta where Rincon Creek empties into the Pacific Ocean at Rincon Point. Thickness of fans in Ojai and at Rincon Point estimated to be at least 15 m

Qia **Intermediate alluvial deposits, undifferentiated (late Pleistocene)—**Undifferentiated unit mapped where poor exposures and geomorphic expression do not allow distinguishing deposits based on relative age. Deposits composed of pale-brown, -tan, and -gray, weakly consolidated silt, sand, and pebble, cobble, and boulder gravel. At most places proportion of gravel greatly exceeds that of sand and silt; a few meters of finer-grained sediments cap alluvial deposits in some exposures. Gravel commonly crudely stratified, and elongate clasts are locally imbricated. Variably rounded gravel clasts mostly composed of locally derived Eocene through Miocene sandstones, siliceous shales and mudstones, and rare reworked cobbles and pebbles derived from conglomerates of the Sespe Formation. Intermediate alluvial deposits form weakly to moderately dissected stream and river strath terraces as high as about 150 m above adjacent modern floodplains and broad, low-relief, piedmont alluvial aprons. In Oak View area strath terraces are cut into both Tertiary bedrock units and semi-consolidated deposits of conglomerate of Ojai (Qco). In piedmont areas average clast size in deposits generally decreases away from bedrock mountain fronts and uplands.

Rockwell and others (1984) estimated late Pleistocene ages (~16–100 ka) for deposits forming elevated ancestral Ventura River terraces in eastern part of map area (units Qia2, Qia3, Qia4, Qia5, and Qia6 of the present map, described below) using radiocarbon ages and estimated rates of faulting of older elevated terraces. These radiocarbon ages were later confirmed, with minor refinements, using terrestrial cosmogenic nuclide dating techniques (DeVecchio and others, 2012). Late Pleistocene age of unit also likely near southwest corner of map area on coastal plain near Carpinteria, where southern edge of apron formed by intermediate alluvial deposits appears to grade into, or interfingers with, late Pleistocene (45? ka) marine-terrace deposits (Qmt) (Wehmiller and others, 1978).

Intermediate alluvial deposits previously mapped as terrace deposits, younger alluvium, and older alluvium (Upson, 1951); alluvium, old alluvium, and Carpinteria Formation (Lian, 1954); old alluvium and Oak View terrace sequence (Clark, 1982); Oak View terraces "Qt3" through "Qt6c" (Rockwell, 1983; Rockwell and others, 1984); alluvium and older dissected surficial sediments (Dibblee, 1987a,b); alluvial deposits (Tan and Clahan, 2004); and alluvial and colluvial deposits (Tan and Jones, 2006). Thickness of intermediate alluvial deposits mostly less than 10 m and thins to a few meters or less where deposits form strath terraces; maximum thickness of deposits may be significantly greater where they underlie broad piedmonts in Ojai and Santa Ana Valleys and on the coastal plain near Carpinteria.

In Ventura River-San Antonio Creek area and along the Los Sauces and Rincon Creeks, terrace-forming intermediate alluvial deposits are subdivided into six age groupings (described below) based chiefly on relative levels (elevations) of terraces and secondarily on degree of erosional dissection and soil development. Terrace-level groupings in Ventura River area approximately follow those of Rockwell (1983) and Rockwell and others (1984), who determined that terrace relative elevations, amount of dissection, and soil maturity all increase with age. In general, terraces on east and west sides of Ventura River are progressively younger towards the modern river floodplain. Deposits assigned to any one terrace level are likely somewhat diachronous and may temporally overlap deposits of younger or older age assignment, both along a single large drainage (for example, Ventura River) and, especially, across breadth of map area

Qia1 **Intermediate alluvial deposits, terrace level 1—**Forms locally preserved terrace remnants a few meters above active (Qa) and Holocene (Qya) alluvial floodplains of San Antonio Creek, Ventura River, and Los Sauces and Rincon Creeks. Weak soil development, with little or no B horizon (Rockwell, 1983). Mostly mapped as Oak View terrace unit "Qt3" by Rockwell (1983)

Qia2 **Intermediate alluvial deposits, terrace level 2—**Forms small to large terrace remnants as much as 15 m above active (Qa) and Holocene (Qya) alluvial floodplains of San Antonio Creek, Ventura River, and Rincon Creek. Weak to moderate soil development (Rockwell, 1983). Mapped as Oak View terrace unit "Qt5a" by Rockwell (1983) and Rockwell and others (1984), who estimated age of terrace level as 16–22 ka

Qia3 **Intermediate alluvial deposits, terrace level 3—**Forms small to large terrace remnants as much as 25 m above active (Qa) and Holocene (Qya) alluvial floodplains of San Antonio Creek, Ventura River, and Rincon and Gobernador Creeks. Moderate soil development (Rockwell, 1983). Mostly mapped as Oak View terrace unit "Qt5b" by Rockwell (1983) and Rockwell and others (1984), who estimated age of terrace level as about 32 ka

Qia4 **Intermediate alluvial deposits, terrace level 4—**Forms small to large terrace remnants as much as 60 m above active (Qa) and Holocene (Qya) alluvial floodplains of Ventura River and Rincon, Gobernador, and Carpinteria Creeks. Moderate to strong soil development (Rockwell, 1983). Mapped as Oak View terrace unit "Qt6a" by Rockwell (1983) and Rockwell and others (1984), who determined age of terrace level as 40 ^{14}C cal ka B.P.

Qia5 **Intermediate alluvial deposits, terrace level 5—**Forms small to large terrace remnants as much as about 85 m above active (Qa) and Holocene (Qya) alluvial floodplains of San Antonio Creek, Lion Creek (near the Lion Fault), Ventura River, and Rincon Creek. Moderate to strong soil development (Rockwell, 1983). Mostly mapped as Oak View terrace unit "Qt6b" by Rockwell (1983) and Rockwell and others (1984), who estimated age of terrace level as 56±10 ka

Qia6 **Intermediate alluvial deposits, terrace level 6—**Forms small to large terrace remnants as much as about 140 m above active (Qa) and Holocene (Qya) alluvial floodplains of San Antonio Creek and Ventura River, and caps Shepard Mesa west of Rincon Creek. Moderate to strong soil development (Rockwell, 1983). Mapped as Oak View terrace unit “Qt6c” by Rockwell (1983) and Rockwell and others (1984), who estimated age of terrace level as 94±13 ka

Qoa **Older alluvial deposits (late? and middle? Pleistocene)—**Nonmarine brown, pale-gray, pale-tan, and reddish-brown, moderately consolidated, crudely stratified, poorly sorted, clayey to silty and pebbly sand and sandstone, silty to sandy pebble-cobble-boulder gravel, conglomerate, and breccia, and rare interbeds and partings of sandy to pebbly clay, silt, and mudstone. Sand and sandstone in places well bedded and cross laminated. Gravel and conglomerate typically occupy paleochannels or form lenticular beds, and contain subrounded clasts composed primarily of sandstone derived from Eocene formations (including Coldwater Sandstone [Tcw]) exposed in Santa Ynez Mountains north of and within map area. Clasts commonly are imbricated. Breccia deposits contain subangular clasts mainly of Eocene sandstone and typically form thick (>3 m), sheet-like, clast-supported beds probably deposited as debris flows.

Older alluvial deposits present chiefly in west part of map area where they form moderately steep and dissected uplands and lower, gently sloping hills along south flank of Santa Ynez Mountains and bordering eastern end of Santa Barbara coastal plain. Deposits interpreted as erosional remnants of old alluvial fans formed along lower flank of Santa Ynez Mountains. Clast size generally decreases and sorting increases away from mountain front. Finer-grained facies at places forms badlands topography. In west part of map area, older alluvial deposits are deformed by youthful faults and upwarps.

Older alluvial deposits also mapped in Santa Ana Valley in northeastern part of map area, where they are preserved as a discontinuous belt of low rounded hills whose surfaces are strewn with cobbles and boulders up to several meters in diameter of Eocene(?) sandstone. In the same area, base of map unit consists of rounded cobble-pebble gravel where it laps onto rocks of the Sespe Formation (Tspu) in a road cut exposure east of Poplin Creek. Nearby, unit inferred to be gently folded into east-plunging syncline near trace of Arroyo Parida fault at west end of valley, based on its arcuate map pattern. At most places in west part of map area, older alluvial deposits overlie dipping strata of the Casitas Formation (Qca) with little or no angular discordance. The deposits closely resemble, and may be partly correlative with, some sediments of the Casitas Formation and the conglomerate of Ojai (Qco). Older alluvial deposits can be distinguished from nearby Casitas deposits by the relatively lesser consolidation and competency of the former. Also, the older alluvial deposits generally contain a smaller percentage of Sespe sandstone clasts and reworked Sespe conglomerate clasts, are more uniform in color, and at some places are less tilted than directly underlying Casitas deposits. Most older alluvial deposits of this report previously mapped as terrace deposits and Casitas Formation (Upson, 1951); Casitas Formation and Carpinteria Formation (Lian, 1954); older dissected surficial sediments (fan gravel and fanglomerate deposits) (Dibblee, 1987a); and alluvial deposits (Tan and Clahan, 2004). Stratigraphic intervals within older alluvial deposits yield significant quantities of groundwater in wells on the Santa Barbara coastal plain west of map area, where unit forms one of the principal aquifer units (Upson, 1951; Muir, 1968).

Maximum age (middle(?) Pleistocene) of unit constrained by middle Pleistocene strata of uppermost Santa Barbara Formation (Qsb) that interfinger with deposits of the Casitas Formation (Qca) in map area, which in turn directly underlie older alluvial deposits; minimum age (late(?) Pleistocene) of unit constrained by elevated, late Pleistocene marine-terrace deposits (Qmt) that lap onto distal facies of older alluvial deposits near southwest corner of map area. Maximum exposed thickness approximately 350 m beneath Shepard Mesa in western part of map area

MARINE-SHORE DEPOSITS

Qb **Beach deposits (Holocene)—**Modern, unconsolidated marine-shoreline beach sediment, mostly fine- to medium-grained, well-sorted, clean, light-grayish-tan sand composed predominantly of quartz, feldspar, and lithic grains. Includes subordinate wave-rounded pebbles, cobbles, and shell fragments, as well as plant remains and litter left by people. Thickness of deposits probably rarely exceeds 5 m and varies seasonally mainly due to storm-surge beach erosion; occasionally during the winter months sand is completely stripped away in places, exposing the underlying bedrock surface that is commonly littered with wave-rounded cobbles. Beach deposits present intermittently along shoreline near southwest corner of map area

Qmt **Marine-terrace deposits (late Pleistocene)—**Mostly pale- to medium-tan and -gray, weakly to moderately consolidated, crudely to moderately bedded, pebble-cobble gravel, pebbly to gravelly sand, and silt. Deposits unconformably overlie elevated marine wave-cut platforms abraded on bedrock. Lower part of marine-terrace sequences typically consists of thin (≤1 m) basal layer of fossiliferous rounded cobble and pebble gravel that locally grades upward into laminated to massive beach(?) sand and (or) estuarine organic-rich clay and silt. Some basal gravel clasts exhibit mollusk (pholad) borings. Upper two-thirds or more of terrace sequences consists of nonmarine eolian sand and silt, stratified alluvial pebble-cobble gravel, and minor colluvial deposits.

Marine-terrace basal-abrasion surfaces in map area are inferred to have formed during interglacial sea-level high stands, whereas the overlying terrace deposits most likely accumulated during marine regressions resulting from eustatic drops in sea level and (or) tectonic uplift (Rockwell and others, 1992; Muhs and others, 1992; Gurrola and others, 2001).

Marine-terrace deposits, exposed in upper part of sea cliffs and U.S. Highway 101 road cuts near southwest corner of map area, are inferred to underlie small, locally dissected coastal mesas that extend inland from the cliffs. The first emergent marine terrace exposed in sea cliff at Carpinteria at 15 m (40–60 ft) elevation (just west of map area; see Minor and others, 2009) continues eastward into map area, where it gradually climbs in elevation eastward and projects across Highway 101 and Rincon Creek into a flight of terraces northeast of Rincon Point. The lower part of this terrace sequence and its associated marine-terrace deposits are expressed by four lower bench-like surfaces separated by subtle (<1 to 2 m height) risers or steps inferred to mark approximate positions of marine shoreline angles (that is, base of paleo sea cliffs); these shoreline angles have approximate elevations of 61 m (200 ft), 73 m (240 ft), 88 m (290 ft), and 116 m (380 ft) above modern sea level. More elevated and dissected, presumably older, marine-terrace deposit remnants present just to the north are bounded by at least two inferred shoreline angles ranging in elevation from 146 to 162 m (480 to 530 ft) (lower shoreline) and 183 to 226 m (600 to 740 ft) (upper shoreline). Eastward-ascending lower part of terrace sequence spanning the Carpinteria-Rincon Point coastal strip has been correlated with the uplifted Punta Gorda terrace preserved east of the map area, which has an amino-acid-racemization estimated age of 45 ka (oxygen isotope stage 3) (Wehmiller and others, 1978; Lajoie and others, 1979; Yerkes and Lee, 1987).

Alluvial deposits typically present in upper part of marine terrace sequences are probably correlative with intermediate alluvial deposits (Qia). Marine-terrace deposits are inferred to grade into, or interfinger with, intermediate alluvial deposits just north of Highway 101 at east end of coastal plain near Carpinteria. Marine-terrace deposits of this report have been previously mapped as terrace deposits (Upson, 1951; Lian, 1954); Carpinteria Formation (Lian, 1954); older dissected surficial sediments (alluvial deposits) (Dibblee, 1987a); and paralic deposits (Tan and Clahan, 2004). Maximum thickness of lower, marine part of terrace deposit sequence approximately 5 m; composite thickness of marine-terrace deposits, including upper nonmarine part, typically ranges from 5 to 10 m

MASS-WASTING DEPOSITS

Qdf **Debris-flow deposits (Holocene and late Pleistocene?)—**Massive, weakly-to moderately-consolidated, poorly sorted, generally matrix-supported rock-debris breccia. Mainly located in southern part of map area on flanks of Rincon Mountain and smaller hills to the east. Chiefly composed of clay, silt, and shale, mudstone, siltstone, and (or) sandstone debris derived from Rincon Shale (Tr), Santa Barbara Formation (Qsb), and (or) Sespe Formation (Tspu, Tspm) exposed upslope.

Youthful lobate and hummocky geomorphic expression of most deposits suggests they are Holocene in age, but considerable erosional dissection of a few deposits suggest some debris flows were emplaced during the late Pleistocene. Most mapped deposits estimated to be less than 10 m thick

Qls **Landslide deposits (Holocene and late? Pleistocene)—**Deposits of diverse slope-movement processes including earth slides, earth flows, rock slides, debris slides, and rock slumps (Bezore and Wills, 2000; terminology of Cruden and Varnes, 1996). Deposits range from poorly sorted, disrupted mixtures of rock fragments and soil to relatively intact bedrock slide blocks. Surfaces of deposits commonly hummocky; downslope-facing breakaway or headwall scarps identifiable and mapped in places. Slopes underlain by Rincon Shale (Tr), Monterey Formation (Tml, Tmu), and relatively fine-grained intervals of the Sespe Formation (Tspu, Tspm, Tspl) and Santa Barbara Formation (Qsb) are particularly susceptible to sliding. Many of the mapped landslide deposits are actually a composite of several smaller overlapping and (or) inset slide units, each formed by one or more episodes of downslope movement. Partial or complete boundaries of slide units mapped where identified within large slide complexes on north and south flanks of Rincon Mountain (southwest part of map area) and on northwest flank of Sulphur Mountain (eastern part of map area). “Landslide” scarps mapped within bedrock units indicate places of incipient or partial break-away and downslope movement of bedrock; laterally most such scarps can be traced into intact (non-slide) bedrock, and bedrock below scarps does not appear to be noticeably disturbed and detached. Bedding attitudes shown on map within landslide deposits indicate places where semi-coherent bedding was measured within large bedrock slide blocks; landslide attitudes document disruption of local bedrock strata due to landslide movement. Slide complex located on south flank of Rincon Mountain along southern border of map area is part of the late Pleistocene Rincon Mountain “megaslide” as inferred by Gurrola and others (2010). Late Pleistocene age of some landslide deposits suggested by their relatively high degree of stream dissection that has locally resulted in perched (relative to modern valley floors) distal ends of the slide deposits. Maximum thickness of deposits in large slide complexes likely exceeds 50 m

BEDROCK UNITS

Qca **Casitas Formation (middle? Pleistocene)—**Nonmarine interbedded conglomerate and gravel, sandstone and sand, siltstone and silt, and rare mudstone forming mostly thin to thick lenticular beds. Formation typically moderately to well consolidated. Deposits in aggregate exhibit pale to medium shades of buff, tan, red, maroon, gray, brown, and, less commonly, green, yellow, and orange, and they commonly form badlands topography where exposed in cliffs.

Conglomerate and gravel contain subrounded to rounded pebbles, cobbles, and boulders, combined in various proportions, in a clayey, silty, and (or) sandy matrix; deposits are both clast-supported and matrix-supported. Conglomerate and gravel deposits are massive to moderately well stratified, in places appear to fill paleochannels, and form beds that locally exceed 5 m in thickness. Clasts composed chiefly of locally(?) derived Eocene and Oligocene (Tcw, Tspl, Tspm, and Tspu) sandstone and lesser siltstone, shale, and mudstone; clasts in upper part of unit east of Rincon Creek also include subangular-to-subrounded pebbles and cobbles of Monterey siliceous shale and mudstone (Tml?, Tmu). Subordinate well-rounded pebbles and cobbles of various other lithologies within the Casitas are probably reworked from conglomerates of the middle and lower units of the Sespe Formation (Tspm, Tspl).

Sandstone and sand are typically pale shades of buff, tan, gray, and greenish-gray, fine to coarse grained, silty, clayey and (or) pebbly, and massive to well bedded and laminated. Sandstone is mostly friable, but locally is well indurated where cemented with carbonate minerals. In places sandstone and sand contain conglomeratic and gravelly lenses.

Siltstone and silt are commonly pale gray and pale greenish-gray, sandy to clayey, and thinly bedded and laminated. Mudstone is commonly brown and forms thin beds and partings. Finer-grained intervals in Casitas, dominated by fine-grained sandstone, siltstone, and mudstone, are as thick as 5 m.

Casitas Formation was first defined and mapped by Upson (1951), who designated type section in western part of map area near confluence of Rincon and Casitas Creeks. Unit subsequently mapped in the Carpinteria-Rincon Creek area as Casitas Formation (Lian, 1954; Dibblee, 1987a; Tan and Clahan, 2004).

Deposits of Casitas Formation are mapped only in the western, coastal area near Rincon Creek and in low hills northeast of Carpinteria. Casitas deposits closely resemble, and may be temporally equivalent with, some of the older alluvial deposits (Qoa), particularly where the alluvial deposits directly overlie Casitas sediments in the low hills and mesas northeast of Carpinteria. The two units can be distinguished, however, by the generally greater amount of clay and silt in Casitas deposits, which results in their somewhat greater consolidation, induration, and competency. Also, Casitas deposits contain a greater percentage of Sespe sandstone clasts and reworked Sespe conglomerate clasts, exhibit a greater variety of colors, and at some places are more strongly tilted than directly overlying older alluvial deposits. Casitas sediments were likely deposited as alluvium shed off of the Santa Ynez Mountains and other nearby uplands. Casitas Formation may be correlative with the similar conglomerate of Ojai (Qco) exposed in eastern part of map area and with nonmarine deposits in the Ventura area (~10 km south of map area) mapped as upper part of San Pedro Formation (Yerkes and others, 1987) and Saugus Formation (Dibblee, 1988). Age of Casitas Formation in map area is bracketed by underlying and interfingering middle Pleistocene upper part of the Santa Barbara Formation (Qsb), and by late Pleistocene marine terrace (Qmt) and intermediate alluvial deposits (Qia) that unconformably overlie it west of Rincon Creek. Maximum exposed thickness ~975 m in area of type section south of Casitas Creek and east of Rincon Creek. Unit also present in subsurface of the coastal plain in the Carpinteria area (Upson, 1951; Jackson and Yeats, 1982). The abandoned Summerland oil field 10 km west of map area produced from sand-rich intervals within Casitas Formation (Arnold, 1907), indicating potential for at least part of formation to serve as a subsurface hydrocarbon reservoir. Coarser-grained intervals within the Casitas yield significant quantities of groundwater in wells and the formation forms one of the principal aquifer units beneath the Santa Barbara coastal plain near and west of Carpinteria (Upson, 1951; Muir, 1968)

Qco **Conglomerate of Ojai (middle? Pleistocene)—**Nonmarine interbedded conglomerate and gravel, sandstone and sand, and subordinate siltstone and silt and rare mudstone forming mostly thin to thick lenticular beds. Deposits in aggregate typically exhibit pale to medium shades of tan, tannish-gray, and brown. Unit mostly moderately to well consolidated and poorly exposed, forming gullied slopes and rounded hills.

Conglomerate and gravel contain subrounded to well-rounded pebbles, cobbles, and boulders, combined in various proportions, supported in a silty and (or) sandy matrix. Conglomerate and gravel deposits are massive to moderately well stratified, in places forming beds and paleochannels that locally exceed 5 m in thickness. Clasts composed chiefly of locally(?) derived, Eocene and Oligocene (Tcw, Tspl, Tspm, and Tspu) sandstone and lesser siltstone, shale and mudstone; rare clasts of shale and mudstone of Monterey Formation (Tml, Tmu) also present locally. Subordinate well-rounded pebbles and cobbles of various other lithologies within the conglomerate of Ojai are probably reworked from conglomerates of middle and lower units of Sespe Formation (Tspm, Tspl). In some beds elongate cobbles and small boulders as much as 0.5 m diameter are crudely to strongly imbricated. Along Lion Creek near the eastern border of map area, conglomerate is anomalously cohesive and dark gray where it is impregnated with tar in the footwall of the Lion fault.

Sandstone and sand are typically pale shades of buff, tan, and tannish-gray, fine to coarse grained, silty, clayey and (or) pebbly, and massive to well stratified and laminated. Sandstone is mostly friable to weakly indurated. In places sandstone and sand contain conglomeratic and gravelly lenses. Sandy and sandstone-rich intervals in places exceed

3 m in thickness. In lower 2–3 m of Highway 33 cut at southern edge of Oak View, conglomeratic deposits of unit overlie massive, mottled (bioturbated?), friable, well-sorted, fine-grained sand atypical of sand layers elsewhere in map unit; this sand interval resembles sandy facies of Santa Barbara Formation (Qsb) exposed in western part of map area, but is lacking any fossil marine shell fragments; lower exposed sand not mapped separately due to its limited, isolated exposure.

Subordinate siltstone and silt are commonly pale gray and pale tannish-gray, sandy to clayey, and thinly bedded and laminated. Rare mudstone is commonly brown to tan and forms thin beds and partings. Finer-grained beds and intervals rarely exceed 1 m in thickness.

Deposits mapped herein as conglomerate of Ojai previously mapped as the Oak View terrace sequence (Clark, 1982); older gravel (Rockwell, 1983); older dissected fan gravel or fanglomerate (Dibblee, 1987b); undivided alluvial deposits (Tan and Jones, 2006); and Saugus Formation (DeVecchio and others, 2012).

Conglomerate of Ojai is exposed only in the eastern part of map area chiefly in the gentle uplands between the Ventura River and San Antonio Creek. Deposits closely resemble, and may be temporally equivalent with, some of the older alluvial deposits (Qoa) mapped to the northwest in western Santa Ana Valley and in the western part of map area near Carpinteria. Conglomerate of Ojai may also be correlative with similar deposits of the Casitas Formation (Qca) mapped in western part of map area and with nonmarine deposits in the Ventura area (~10 km south of map area) mapped as upper part of San Pedro Formation (Yerkes, Sarna-Wojcicki, and Lajoie, 1987) and Saugus Formation (Dibblee, 1988). Conglomerate of Ojai was likely deposited as alluvium shed off of the Santa Ynez Mountains, Topatopa Mountains, and other nearby uplands. Age of conglomerate of Ojai in map area is not well constrained, bracketed by unconformably underlying Miocene Monterey Formation (Tml, Tmu), and by oldest preserved late Pleistocene intermediate alluvial deposits (Qia6) unconformably overlying it. Middle(?) Pleistocene age inferred from possible correlation with Casitas Formation deposits to west, which overlie middle and early Pleistocene Santa Barbara Formation (Qsb), and with deposits of the upper part of San Pedro Formation to south near Ventura having an estimated age of ~200 ka (Yerkes, Sarna-Wojcicki, and Lajoie, 1987). Maximum exposed thickness in map area ~130 m; a maximum unit thickness of 240 m was determined by McKay (2011), using water well data of Kear (2005), in subsurface of Ojai Valley about 7 km northeast of the map area. Coarser-grained intervals within the conglomerate of Ojai have the potential to yield significant quantities of groundwater in wells and may form a significant aquifer beneath Ojai Valley and the Oak View-Ventura River area (Kear, 2005)

Qsb **Santa Barbara Formation (middle and early Pleistocene)—**Marine fossiliferous sandstone with subordinate siltstone, mudstone, and conglomerate. Sandstone is mostly pale-gray and cream-colored (fresh) to buff and shades of pale-tan, -yellow, and -gray (weathered), fine- to medium-grained, and includes silty, clayey, and pebbly beds and intervals. Sandstone ranges from bioturbated and massive to crudely or moderately bedded and planar- to cross-laminated. Sandstone is mostly friable, but includes rare resistant sandstone beds that are cemented with carbonate minerals. White to gray fossil marine shell fragments are common within sandstone, both in isolated occurrences and concentrated in layers of shell hash.

Siltstone, mudstone, and rare shale weather pale-gray and pale-greenish-gray, are typically laminated, and form partings, interbeds, and thin-bedded intervals that are commonly accompanied by silty to clayey fine-grained sandstone beds.

Conglomerate and conglomeratic sandstone, which weather to tannish-red brown to rusty-orange brown, form paleochannels, lenses, beds, and intervals as thick as ~10 m. Conglomerates are polymict, containing generally well-rounded pebbles and subordinate cobbles composed of sandstone possibly derived from Eocene formations exposed in nearby Santa Ynez Mountains (including Tspl, Tcw), chert and intermediate-to-silicic volcanic rocks possibly reworked from conglomerates of the Sespe Formation (Tspm, Tspl), shale and mudstone of the Monterey Formation (Tmu?, Tml?), and other rock types of uncertain provenance.

Diverse marine invertebrate fossil assemblages, dominated by mollusks, are concentrated in multiple stratigraphic intervals within exposed part of Santa Barbara section, ranging in thickness from less than 1 m to several tens of meters. Most shells are disarticulated, fragmented, and concentrated in beds and lenses in both sandstone and finer-grained intervals. Unit includes rare, whitish beds of calcareous coquina.

Santa Barbara Formation is exposed only in Rincon Creek area in west part of map area, where a moderate to pronounced angular unconformity separates formation from underlying Miocene units (Tr, Tml, Tmu). Surface trace of this unconformity east of Rincon Creek, on lower western flank of Rincon Mountain, marks eastern limit of exposure (and possibly deposition) of unit. Upper contact of Santa Barbara Formation with overlying Casitas Formation (Qca) is gradational where exposed in low hills east of Rincon Creek, expressed by ~35-m-thick interval of interfingering or interstratified Santa Barbara-like marine (fossil-shell bearing) sandstones and Casitas-like conglomerates and sandstones. Upper contact mapped at top of stratigraphically uppermost bed of fossiliferous marine sandstone.

Molluscan fossils collected from Santa Barbara Formation in southwestern-most part of map area and on Santa Barbara coastal plain west of map area (Minor and others, 2009) examined by C.L. Powell, II (USGS, written commun., 2001) characteristically include bivalves *Chlamys* spp., *Cyclocardia occidentalis* (Conrad), *C. californica* (Dall), *Humilaria perlaminosa* (Conrad), *Lucinoma annulatum* (Reeve), *Patinopecten caurinus* (Gould), *Pecten bellus* (Conrad), and gastropods *Amphissa reticulata* (Dall), *Boreotrophon* spp., *Crepidula princeps* (Conrad), *Olivella biplicata* (Sowerby), *Neptunea tabulata* (Baird), and *Turritella cooperi* Carpenter. The molluscan fauna are consistent with deposition at shelf water depths and a possible late Pliocene to middle Pleistocene age (C.L. Powell, II, written commun., 2001). Previously, Dibblee (1966) presented a list of molluscan fossils from the formation interpreted to indicate a “late Pliocene(?) to early Pleistocene” age.

Middle and early Pleistocene age provisionally assigned to Santa Barbara Formation in this report based partly on reconnaissance paleomagnetic data from Santa Barbara coastal plain west of map area. These data suggest that much of formation was deposited during the normal polarity epoch following the Brunhes-Matuyama geomagnetic reversal at about 780 ka (Keller and Gurrola, 2000; Gurrola and others, 2001; J.W. Hillhouse, USGS, written commun., 2007). Middle and early Pleistocene age also consistent with (1) a reported amino-acid racemization age of 500–600 ka for formation ~ 20 km west of map area (Wehmiller, 1992), (2) strontium isotopic data suggesting an age of 400–900 ka for formation near Santa Barbara Harbor ~20 km west of map area (Patterson and others, 1990), (3) age of about 600 ka for planktic foraminifer *Neogloboquadrina pachyderma* within formation near Santa Barbara Harbor (Patterson and others, 1990), and (4) a 1.2 Ma (Mega-annum, million years) age determination for the Bailey ash (Izett, Naeser, and Obradovich, 1974), which directly underlies Santa Barbara Formation in the Ventura area ~8 km south of map area (Yerkes, Sarna-Wojcicki, and Lajoie, 1987).

Unit typically is poorly exposed and forms subdued rounded hills except in some narrow, steep-walled stream canyons where soil and regolith have been stripped off of Santa Barbara rocks; silt- and clay-rich intervals locally erode into badlands topography. Formation has a minimum thickness of approximately 350 m east of Rincon Creek; upper part of section in this area is truncated by the Rincon Creek fault.

Unit was also mapped as Santa Barbara Formation by earlier workers (Upson, 1951; Lian, 1954; Dibblee, 1987a; Tan and Clahan, 2004). Coarser-grained intervals within the unit yield significant quantities of groundwater in wells and the Santa Barbara Formation forms one of the principal aquifer units beneath the Santa Barbara coastal plain (Upson, 1951; Muir, 1968)

Tsq **Sisquoc Formation (lower Pliocene and upper Miocene)—**Marine diatomaceous mudstone and shale, and subordinate dolomite and conglomerate. Distinguished from the underlying upper siliceous unit of the Monterey Formation (Tmu) by abrupt upward change from generally hard, siliceous mudstone and shale to typically pale gray-brown, relatively soft diatomaceous mudstone and, locally, conglomerate.

Diatomaceous mudstone and shale are white to pale-gray and pale-gray-brown weathering, and gray to brown on freshly broken surfaces. Mudstone is generally soft to moderately hard; shale ranges from soft to, rarely, hard and fissile; where moderately hard, both rock types commonly exhibit dense hackly fractures. Both mudstone and shale are generally of conspicuously low density. Reaction in dilute hydrochloric acid (HCl) ranges from weak to strong, indicating the presence of variable amounts of carbonate minerals. Foraminifers, diatoms and diatom debris, and fish scales and other fragments are common to abundant, particularly along surfaces that are broken parallel to stratification; preservation of diatoms is generally poor in the Sulphur Mountain area. Most mudstone and shale beds are moderately to strongly laminated but some are massive and bioturbated. Laminations, generally 0.5–10.0 millimeters (mm) thick, are defined by light and dark color bands. At places, such as in railroad and highway cuts near Rincon Point, shale is impregnated with oil, and at other places densely fractured mudstone exhibits hydrocarbon staining and a petroliferous odor.

Dolomite constitutes less than 1 percent of the formation and forms laterally persistent beds generally less than 50 centimeters (cm) thick, ranging to 100 cm thick, and ellipsoidal to spheroidal concretions as much as about 100 cm in longest dimension. Dolomite is very hard, gray to brown on freshly broken surfaces, weathers pale-gray to light orange, light brown, or ocher, is aphanitic to sugary in texture, and reacts slowly or not at all in dilute HCl. Laminations, mostly 1–10 mm thick but as much as 20 mm thick, are defined by alternating light and dark color banding.

Conglomerate consists mainly of angular to subrounded clasts of mudstone, shale, dolomite, and porcelanite apparently derived from underlying Monterey Formation (Tml and [or] Tmu). Generally, clasts range up to boulders as much as 1 m across, but the largest blocks are more than 5 m across. Laminated clasts typically are oriented at various angles to each other and bedding. However, some large, elongate clasts are parallel or subparallel to stratification. The matrix between the clasts is massive to laminated diatomaceous mudstone. Conglomerate is recognized only in basal ~20-m-thick interval of Sisquoc Formation where exposed in abandoned railroad cut above sea cliff west of Rincon Point; its presence elsewhere within unit is uncertain due to generally poorly exposed nature of unit. In railroad cut, matrix-supported blocks in basal conglomerate include a large (~7-m-wide) block(?) of buff, massive, fine-grained sandstone of unknown provenance.

Sisquoc Formation samples from a coastal exposure near and east of the University of California, Santa Barbara, campus about 30 km west of map area yielded diatoms of the *Thalassiosira miocenica/Nitzschia miocenica* Assemblage Zone (upper Miocene, about 6.2–6.7 Ma) (basal Sisquoc) and of the *Thalassiosira oestrupii* Zone (lower Pliocene, younger than 5.5 Ma) (upper part of Sisquoc) (J.A. Barron, oral and written commun., 2001, 2002, 2005) (see also Minor and others, 2009). In the map area, samples of mudstone and shale from sea cliff and railroad cut near Rincon Point yielded diatoms of the *Thalassiosira praeostrupii* subzone (uppermost Miocene, ca. 5.9–5.5 Ma) (J.A. Barron and R.G. Stanley, written communs., 2005).

Rocks mapped in this study as Sisquoc Formation previously mapped as Monterey Shale (Upson, 1951); Santa Margarita Formation (Lian, 1954); Sisquoc Shale (Dibblee, 1987a,b; Tan and Jones, 2006); and Sisquoc Formation (Tan and Clahan, 2004).

Thickness of Sisquoc Formation in map area is uncertain; where unit is exposed near Rincon Point upper contact is concealed by alluvial fan deposits (Qaf) and (or) is offshore, and where it is present south of Sulphur Mountain upper contact lies outside (south) of map area. Sisquoc is at least 280 m thick in the Rincon Point area and at least 400 m thick on the south upper flank of Sulphur Mountain.

Organic content in Sisquoc is locally great enough in region for unit to qualify as a potential hydrocarbon source (Tennyson and Isaacs, 2001). Sisquoc Formation is generally weakly resistant to erosion and poorly exposed except in cuts and sea cliffs near Rincon Point

Monterey Formation (Miocene)—Marine, predominantly well-bedded, siliceous and calcareous mudstone and shale with subordinate porcelanite and dolomite. The Monterey Formation is well exposed in sea cliffs west of Rincon Point near the southwestern corner of map area and along a small stretch of shoreline it underlies on the west side of Lake Casitas. However, the Monterey generally is poorly exposed and highly weathered, with many original lithologic details obscured, where it crops out inland on the northwest spur of Rincon Mountain, on the northwest flank of Sulphur Mountain, and in low hills on the east side of Lake Casitas and in the Oak View area. The Monterey Formation is of Miocene age on the basis of abundant biostratigraphic data from microfossils (Dibblee, 1966; Ingle, 1980, and references therein; Arends and Blake, 1986; Barron, 1986; DePaolo and Finger, 1991; Blake, 1994; Hornafius, 1994a,b, and references therein). No complete, continuous, tectonically undisrupted sections of the Monterey Formation are exposed in map area; thickest partial sections of Monterey in map area are about 550 m near the mouth of Rincon Creek and about 340 m on the north flank of Sulphur Mountain. Organic contents in rocks of the Monterey Formation are generally high and the unit is a major potential hydrocarbon source in the region (Tennyson and Isaacs, 2001). Also, highly fractured zones within the formation form localized oil reservoirs (Tennyson and Isaacs, 2001).

The Monterey Formation is divided into two subunits in map area that are distinguished from each other by lithology and age: an upper siliceous unit and a lower calcareous unit. The upper siliceous unit (Tmu) consists mainly of diatomaceous mudstone and shale, siliceous shale, and porcelanite. The lower calcareous unit (Tml) consists mainly of calcareous mudstone and shale. Microfossil assemblages, mainly diatoms, calcareous nannofossils, and benthic foraminifers, indicate that the upper unit is of late and middle Miocene age and the lower unit of middle and early Miocene age

Tmu **Upper siliceous unit (upper and middle Miocene)—**Consists mainly of diatomaceous mudstone and siliceous shale with subordinate porcelanite and lesser dolomite and calcareous mudstone and shale. Mudstone and shale generally weather white, cream, and pale tan and are generally pale brown to gray on fresh surfaces. Most rocks are soft to moderately hard, less resistant to weathering than dolomite and porcelanite, and noticeably low density. Generally weak or no reactions to dilute HCl indicate the presence of mostly small to negligible amounts of carbonate minerals. In places, mudstone and shale contain abundant, well-preserved microfossils visible with hand lens, including diatoms, foraminifers, and fish scales and bone fragments. Mudstone and shale generally form flaggy and platy to tabular, thin to medium beds; most beds are less than 30 cm thick, but some are 100 cm thick or more. Mudstone and shale are typically well laminated; laminations are generally planar and 0.5–20 mm thick. Rarely, beds include cream phosphatic laminations and (or) oblate phosphatic nodules as thick as 1 cm, with the longest dimension usually parallel to bedding. Phosphatic laminae and nodules increase in frequency down section towards base of upper siliceous unit. In places, mudstone and shale exhibit hydrocarbon staining and a strong petroliferous odor. Diatomaceous mudstone and shale decrease in abundance down section relative to other lithologic components. Siliceous mudstone and shale present on northwest flank of Sulphur Mountain are harder and more brittle, porcelaneous, and fissile (shale) than elsewhere in map area. Also in this area, rare, thin (<2 cm) layers of black, glassy chert are locally present near base of upper siliceous unit.

Porcelanite and porcelaneous mudstone form isolated, resistant beds as much as 10 cm thick that are sporadically interstratified with diatomaceous mudstone and shale. Porcelanite is hard and brittle, gray to brown on fresh surfaces, weathers pale gray and tan to white, and exhibits conchoidal fracture and porcelaneous luster. Porcelanite is generally well laminated. In places, it is densely fractured and stained by hydrocarbons with a strong petroliferous odor; locally porcelanite is brecciated.

Rare dolomite forms concretions and beds that increase in frequency down section towards basal contact of upper siliceous unit. Concretions are ellipsoidal to spheroidal, generally 10–50 cm thick and less than 2.5 m long, and usually oriented with the long axis parallel to stratification. Beds are generally laterally persistent and mostly about

10–100 cm thick. Dolomite is very hard and brittle, commonly fractured, relatively resistant, brown to gray on fresh surfaces, generally weathers pale orange or yellow orange, and aphanitic to sugary in texture. Reaction of the dolomite in dilute HCl ranges from none to weak.

Calcareous shale and mudstone weather white, cream, and pale gray, tan, and brown, and are generally brown to gray on fresh surfaces. Rocks generally react vigorously in dilute HCl. Most calcareous beds are well laminated; laminations are mostly planar. Calcareous shale and mudstone form thin to medium flaggy to tabular beds that increase in frequency down section towards base of upper siliceous unit.

A single thin (4-cm-thick), pinkish-gray weathering tuff layer is exposed at, or a few meters stratigraphically above, the basal contact of upper siliceous unit in the sea cliff 1.5 km northwest of Rincon Point.

Published biostratigraphic studies of assemblages of diatoms and foraminifers, summarized by Hornafius (1994a,b), show that Monterey rocks approximately equivalent to the upper siliceous unit (as mapped herein) exposed along the coast about 45 km west of map area (Dos Pueblos Canyon area) were deposited about 8.0–14.5 Ma. Samples of upper part of the upper siliceous unit collected in the Santa Barbara area about 17 km west of map area yielded late Miocene diatoms ranging in age from ca. 8.5 to 9.9 Ma (Minor and others, 2009). Within map area in the Rincon Point area, shale samples from uppermost part of upper siliceous unit yielded late Miocene diatoms that are likely younger than 8.6 Ma (that is, lacking *Denticulopsis*) (J.A. Barron and R.G. Stanley, written commun., 2004). Samples of the middle shale unit of the Monterey Formation as mapped by Minor and others (2009) (equivalent to lower part of upper siliceous unit mapped herein) from coastal exposures about 20 km west of map area yielded benthic foraminiferal assemblages indicative of the Mohnian Stage of Kleinpell (1938, 1980) and mostly middle bathyal (500–2,000 m) water depths, as well as calcareous nannofossils of probable late Miocene age (R.S. Boettcher and S.A. Kling, Micropaleo Consultants, written communs., 2001) (see also Minor and others, 2009). Shale and mudstone samples collected in eastern part of map area (northwest flank of Sulphur Mountain) from approximate base of upper siliceous unit yielded middle Miocene benthic foraminiferal assemblages indicative of the Luisian Stage to upper part of Luisian Stage of Kleinpell (1938, 1980) and upper bathyal (150–500 m) water depths (K.A. McDougall, USGS, written commun., 2012).

The upper siliceous unit rests conformably on the lower calcareous unit (Tml). In the sea cliff west of Rincon Point, the contact between the upper and lower units of the Monterey Formation is placed at, or just stratigraphically below, a single conspicuous tuff bed where there is a marked upward increase in the frequency and thickness of siliceous and porcelaneous beds. Inland within the map area the base of upper unit, although poorly exposed, is mapped at a similar abrupt change in lithology.

Rocks assigned herein to the upper siliceous unit previously mapped as Monterey Shale (Upson, 1951; Lian, 1954); upper shale unit of the Monterey Formation (Dibblee, 1987a,b); Monterey Formation (Tan and Clahan, 2004); and upper section of the Monterey Formation (Tan and Jones, 2006). Upper siliceous unit mapped herein equivalent to both the upper siliceous and middle shale units of the Monterey Formation as mapped by Minor and others (2009) on the Santa Barbara coastal plain west of map area; these two units are combined on the present map because field exposures are generally inadequate to differentiate the middle and upper units. Thickness of the upper siliceous unit decreases eastward, from about 360 m near the mouth of Rincon Creek to about 190 m on the northwest flank of Sulphur Mountain. Upper siliceous unit is variably resistant to erosion and moderately to highly susceptible to landsliding. East of San Antonio Creek, on the lower northwest flank of Sulphur Mountain, the upper siliceous unit is involved in several large landslides and landslide complexes (mapped as Qls), many of which compose large translated and partly rotated blocks of internally intact bedrock in which remnants of pre-landslide stratigraphy are preserved. In inland upland areas, upper siliceous unit is generally poorly exposed and mostly covered by colluvium and dense vegetation

Tml **Lower calcareous unit (middle and lower Miocene)—**Calcareous, siliceous, and phosphatic mudstone and shale, with subordinate dolomite, porcelanite, and sandstone. Distinguished from the underlying Rincon Shale (Tr) mainly by its well-bedded character, white-to-tan color, and greater proportion of siliceous shale and mudstone, which typically are harder and more resistant to weathering than Rincon Shale.

Mudstone and shale range from moderately hard to very hard, weather white, pale cream, and pale gray, and are pale brown, brown, and gray brown on fresh surfaces. Mudstone and shale are well stratified and form laterally persistent beds generally 3–30 cm thick, but some beds are as thick as 100 cm. Beds vary considerably in relative resistance to weathering; more resistant beds are commonly tabular or flaggy. Reaction in dilute HCl varies from none to strong and indicates that many beds are moderately to highly calcareous. Most beds exhibit laminations ranging from 0.5 to 10 mm thick, which are defined by subtle variations in color and texture; some beds are massive to bioturbated. Microfossils are locally abundant and consist mainly of calcareous foraminifers and fish scales and fragments. In places, white-to-cream phosphatic nodules and laminae are abundant, generally about 1–10 mm thick and 5–25 cm in longest dimension, which is always parallel to bedding. Intervals of mudstone with abundant phosphatic nodules and laminae appear to be more frequent in the upper part of the unit. These intervals weather white to pale tan, are dark gray to brown on fresh surfaces, and generally are less resistant to weathering than calcareous and siliceous mudstones.

Dolomite is very hard, resistant, weathers yellow gray, orange gray, orange tan, and ocher, and is gray to gray brown on freshly broken surfaces. Dolomite constitutes less than 5 percent of the unit and generally forms beds and concretions about 10–50 cm thick. Concretions are ellipsoidal to irregular in shape and about 1–2 m in longest dimension, which usually parallels stratification. Most dolomite reacts slowly with dilute HCl, but some weathered dolomite reacts strongly. Dolomite beds are commonly densely fractured.

Porcelanite is hard, brittle, resistant, exhibits conchoidal fracture, weathers light gray to white, and is gray to brown on freshly broken surfaces. Porcelanite is present at irregular intervals in the unit as massive to well-laminated beds about 5–20 cm thick that increase in thickness and abundance upward in the unit. Some intervals of porcelanite contain subordinate dolomite interbeds. Thin (1–2 cm) lenses and seams of black, glassy chert are present locally in the lower calcareous unit in the Sulphur Mountain area.

At places along sea cliff and railroad cuts west of Rincon Point the lower calcareous unit includes intervals as thick as 30 m in which beds are gently to moderately folded, faulted, stretched, and brecciated; these intervals exhibit outcrop-scale, disharmonic folds with wavelengths and amplitudes as much as 10 m, discontinuous faults with small offsets, and beds that are stretched and thinned. Breccia consists of angular to subrounded clasts of mudstone, shale, dolomite, and porcelanite in a mudstone matrix; breccia is both clast-supported and matrix-rich, the latter having a mélange-like appearance. Although some of this breccia may have formed due to tectonic deformation well after sediment deposition and lithification, much of it may have formed during downslope, gravity-driven slumping and flow of soft to partly lithified sediment shortly after deposition, possibly in a submarine slope environment (Garrison and Ramirez, 1989).

Sandstone constitutes much less than 1 percent of lower calcareous unit. Sandstone beds weather pale tan to gray, are shades of brown and gray on freshly broken surfaces, and are generally more resistant to weathering than the underlying and overlying horizons of mudstone and shale; beds are tabular to flaggy and range from 10-to-100 cm thick. Sandstone is medium to coarse grained, feldspathic to lithic, and commonly stained with oil; rounded pebbles of dolomite and (or) other lithologies observed in one sandstone bed. Mostly forms single, isolated beds, but one thin (~3 m) mudstone/shale interval exposed in the sea cliff about 2 km northwest of Rincon Point contains three sandstone beds; a separate sandstone bed nearby is accompanied by a small sandstone dike.

Samples of mudstone and shale from the lower calcareous unit in the sea cliff about 1 km west of the map area yielded benthic foraminifers indicative of the Relizian and Saucesian Stages of Kleinpell (1938, 1980) and lower middle bathyal to upper middle bathyal (500–2,000 m) water depths (K.A. McDougall, written commun., 2004), and calcareous nannofossils of lower middle to lower Miocene zones CN4 to CN1

(R.S. Boettcher and S.A. Kling, written communs., 2002, 2003) (see also Minor and others, 2009). In same sea cliff to east within southwestern corner of map area, samples of mudstone and shale from the lower unit yielded benthic foraminifers indicative of the lower part of the Relizian to lower part of Luisian Stages of Kleinpell (1938, 1980) and upper middle to upper bathyal (150–1,500 m) water depths (K.A. McDougall, written commun., 2004), and calcareous nannofossils of lower middle to upper lower Miocene zone CN3 (R.S. Boettcher and S.A. Kling, written communs., 2002, 2003). Farther to the east along same sea cliff, mudstone samples from upper part of lower calcareous unit yielded benthic foraminifers indicative of the Luisian Stage to upper part of Luisian Stage of Kleinpell (1938, 1980) and upper bathyal (150–500 m) water depths (K.A. McDougall and R.G. Stanley, written commun., 2012). In eastern part of map area, a mudstone sample from lower part of lower unit exposed east of Ventura River (just south of Oak View) yielded benthic foraminifers indicative of the Saucesian to Relizian Stages of Kleinpell (1938, 1980) and upper middle bathyal (500–1,500 m) water depths (K.A. McDougall, written commun., 2012). Shale and mudstone samples collected in Sulphur Mountain-San Antonio Creek area (eastern part of map area) from approximate stratigraphic top of lower calcareous unit yielded middle Miocene benthic foraminiferal assemblages indicative of the Luisian Stage to upper part of Luisian Stage of Kleinpell (1938, 1980) and upper bathyal (150–500 m) water depths (K.A. McDougall, written commun., 2012).

The conformable contact between the lower calcareous unit and the underlying Rincon Shale (Tr) is placed at abrupt lithologic transition from well-bedded, white- to cream-weathering calcareous and siliceous mudstone and shale (typical of the lower calcareous unit) to the underlying massive, pale-gray mudstone (typical of the Rincon Shale). In most of map area, however, contact between the lower calcareous unit and the Rincon Shale is covered or poorly exposed.

Strata mapped in this report as the lower calcareous unit previously mapped as Monterey Shale (Upson, 1951; Lian, 1954); lower shale unit of Monterey Formation (Dibblee, 1987a,b); upper shale unit of Monterey Formation (Dibblee, 1987a); Monterey Formation (Tan and Clahan, 2004); and lower section or upper section of the Monterey Formation (Tan and Jones, 2006). Only minimum thicknesses of the lower calcareous unit can be determined in map area due to structural truncations and complications affecting the lower Monterey section; lower unit has a minimum thickness of about 190 m near the mouth of Rincon Creek, about 150 m on the north flank of Sulphur Mountain, and about 250 m in a fault block west of San Antonio Creek. The lower calcareous unit is well exposed along sea cliff and railroad cuts west of Rincon Point, but generally is poorly exposed where present inland on the flanks of Rincon Mountain, in the low hills east of Lake Casitas, in the Oak View area, and on the north flank of Sulphur Mountain. Lower calcareous unit generally is weakly resistant to erosion and moderately to highly susceptible to landsliding. East of San Antonio Creek, on northwest flank of Sulphur Mountain, and on south flank of Rincon Mountain (“Rincon Mountain Megaslide” of Gurrola and others [2010]), the lower unit is involved in several large landslides and landslide complexes (mapped as Qls), many of which compose large translated and partly rotated blocks of internally intact bedrock in which remnants of pre-landslide stratigraphy are preserved. In inland upland areas, lower calcareous unit is generally poorly exposed and mostly covered by colluvium and dense vegetation

Tr **Rincon Shale (lower Miocene)—**Marine mudstone, with subordinate dolomite, sandstone, and conglomeratic sandstone; locally fossiliferous. More than 90 percent of the Rincon Shale is composed of mudstone that is gray to gray brown on freshly broken surfaces, weathers pale gray, olive gray, greenish gray, and rusty brown, is generally hard to moderately hard, and generally shows a moderate to weak reaction in dilute HCl. Mudstone typically exhibits dense hackly and, less commonly, spheroidal fractures and forms a distinctive pale greenish-gray, granular, clay-rich soil. At places, the mudstone contains abundant microfossils including calcareous foraminifers and fish scales, and some mudstone and sandy mudstone beds near basal contact with Vaqueros Formation (Tv) contain fossil oyster and other marine shells. Rare red-brown ferruginous(?) mudstone beds present in some exposures. Mudstone is generally massive and bioturbated and thick bedded, with beds generally 30–200 cm thick.

Dolomite is hard, resistant to weathering, gray to gray brown on freshly broken surfaces, weathers to shades of orange, yellow orange, and orange brown, has aphanitic to sugary texture, and reacts slowly or not at all in dilute HCl. Dolomite forms laminated to massive, laterally-persistent beds as thick as 100 cm, and also spheroidal to ellipsoidal concretions that range in size from a few centimeters to nearly 3 m across. The long axes of the dolomite concretions commonly parallel bedding.

Sandstone forms sparse to rare interbeds within thick sequences of mudstone. Sandstone chiefly weathers shades of gray and is medium to fine grained and commonly clayey and calcareous. Sandstone interbeds are generally tabular, resistant, 5–40 cm thick, laterally persistent, and increase in frequency both eastward and down section as contact with Vaqueros Formation (Tv) is approached. Some thick (~3 m) sandstone beds near San Antonio Creek in eastern part of map area are coarse grained and conglomeratic, containing rounded pebbles and small cobbles possibly reworked from Sespe (Tspm) conglomerates; other sandstone beds and intervals in this area are fossiliferous, containing abundant oyster, gastropod, and other shells.

Tuff layer(s) exposed in the Rincon Shale at two localities in the Summerland area (about 10 km west of the map area; see Minor and others [2009] for specifics and references) yielded $^{40}Ar/^{39}Ar$ and K-Ar ages ranging from 16.5 to 17.3 Ma. The age of the Rincon Shale in the map area is considered to be early Miocene on the basis of these isotopic ages and previously reported Saucesian benthic foraminifers and other biostratigraphic evidence from: (1) the Rincon type section along Los Sauces Creek in and directly south of south-central part of map area (Kleinpell, 1938), and (2) a measured stratigraphic section in Cañada de la Pila, about 63 km west of map area (Stanley and others, 1992, 1994). Base of the Rincon Shale is considered to be coincident with the Oligocene-Miocene boundary (David Bukry, USGS, oral commun., 1994).

Upper contact of the Rincon Shale is mapped at base of lowermost bed or interval of white- to cream-weathering shale and mudstone of conformably overlying lower calcareous unit of the Monterey Formation (Tml). Basal contact is mapped at top of uppermost bed or interval of feldspathic sandstone typical of the conformably underlying Vaqueros Formation (Tv).

Unit previously mapped as Rincon Formation (Lian, 1954) and Rincon Shale (Upson, 1951; Dibblee, 1987a,b; Tan and Clahan, 2004; Tan and Jones, 2006). The Rincon Shale is about 470 m thick near its type section south of Casitas Valley along Los Sauces Creek. Organic contents in the Rincon Shale are generally high enough for the unit to qualify as an important potential hydrocarbon source in the region (Tennyson and Isaacs, 2001). The unit is generally poorly exposed and covered by vegetation where present in the uplands along the southern border of the map area, east of Lake Casitas, and south of Ojai Valley. The Rincon Shale is extremely susceptible to landsliding (Bezore and Wills, 2000), for example on the northwest flank of Rincon Mountain in the southwest part of map area, where a large landslide complex is mapped

Tv **Vaqueros Formation (upper Oligocene)—**Shallow-marine sandstone; pale tan, gray, and greenish-gray, moderately to well indurated, feldspathic, and locally fossiliferous. Sandstone is typically cemented with carbonate and moderately to strongly resistant to erosion, locally forming prominent ledges, cliffs, and ridges; commonly weathers to pale-tan and -gray, rounded sandstone outcrops and distinctive, pale-tan, sandy soils; some outcrops exhibit cavernous weathering. Sandstone locally is mottled tan and greenish gray. Sandstone ranges from massive and bioturbated to laminated, from thick to thin (tabular) bedded, and from fine to coarse grained. Both planar and cross laminations are common. Rare thin (5–15 mm) partings of gray siltstone and mudstone also present. Uppermost part characterized by interbedded, thinly laminated sandstone, siltstone, and mudstone; ratio of mudstone-siltstone to sandstone increases towards stratigraphic top of Vaqueros; some sandstone beds near top of unit are coarse grained, pebbly (including chert clasts), and rich in shell fragments. Upper contact mapped at top of uppermost prominent bed or interval of relatively pure (that is, low clay content) sandstone. Base of unit is typically marked by a distinctive thin (0.5–2 m) interval of well-indurated and flaggy, thinly bedded and laminated, pale-gray, calcareous sandstone containing abundant pelecypod and other shell fragments and, locally, rounded pebbles of chert and other lithologies. Basal contact is sharp and recognized by abrupt change from thick, tan-gray sandstone and basal gray, shell-rich sandstone of the marine Vaqueros to underlying maroon to greenish-gray, interbedded, tabular sandstone and mudstone of the nonmarine Sespe Formation.

Late Oligocene age of Vaqueros Formation is inferred from stratigraphic position of unit, which overlies upper Oligocene upper part of Sespe Formation and underlies lower Miocene Rincon Shale. Base of overlying Rincon Shale is considered to be approximately coincident with the Oligocene-Miocene boundary (David Bukry, oral commun., 1994). Rigsby (1998) reported a strontium-isotope date of 24±1 Ma from oyster shells in Vaqueros Formation in Hollister Ranch area 85 km west of map area, consistent with late Oligocene (or earliest Miocene) age.

Unit previously mapped as Vaqueros Sandstone (Upson, 1951; Lian, 1954; Dibblee, 1987a,b; Tan and Jones, 2006) and Vaqueros Formation (Tan and Clahan, 2004). In map area unit increases in thickness eastward, from about 25 m in Casitas Valley and Lake Casitas area to about 90 m just west of Ventura River; a regional thickness of about 100 m was reported by Dibblee (1982). Some oil in the region is produced from Vaqueros sandstone reservoirs (Tennyson and Isaacs, 2001)

Sespe Formation (Oligocene and upper Eocene)—Nonmarine, fluvial sandstone, mudstone, and conglomerate; predominantly maroon, reddish-brown, and greenish- to pinkish-gray. The poorly to moderately exposed Sespe Formation is present over a large portion of the map area in the foothills north of Carpinteria, in the Laguna Ridge area, and in the hills and uplands surrounding Santa Ana and Ojai Valleys. The Sespe is divided into three subunits that are distinguished from each other mainly by differences in lithology, provenance, and age: an upper sandstone and mudstone unit (Tspu), a middle conglomerate and sandstone unit (Tspm), and a lower conglomerate and sandstone unit (Tspl). A major distinguishing feature of the upper unit is its lack of conglomerate, whereas the conglomeratic middle and lower units are distinguished mainly by their differing clast compositions and colors of weathered sandstone and conglomerate beds (mostly maroonish shades in middle unit and pinkish- to tannish-gray shades in lower unit). In the map area, the middle unit composes well over half of the total thickness of formation. Overall thickness of Sespe Formation is more than 1,600 m in the Laguna Ridge area. Some oil in the region is produced from Sespe sandstone and conglomerate reservoirs (Tennyson and Isaacs, 2001).

Age of Sespe Formation in the map region is considered late Eocene and Oligocene by Howard (1995), with an intraformational unconformity representing much or all of early Oligocene time. This unconformity (erosional disconformity) coincides with the mapped contact separating the lower conglomerate and sandstone unit (Tspl) from the middle conglomerate and sandstone unit (Tspm). Rocks below unconformity have been interpreted as part of an upper Eocene to lowermost Oligocene fluvial sequence composed of clastic detritus derived primarily from bedrock now exposed in the Mojave Desert, whereas overlying rocks have been interpreted as part of a lower(?) and upper Oligocene fluvial sequence containing chert, graywacke, and other clasts derived from Franciscan Complex source terrane(s) (Howard, 1995)

Tspu **Upper sandstone and mudstone unit (upper Oligocene)—**Sandstone, siltstone, and mudstone interbedded in proportions that vary both laterally and through the section; sandstone to mudstone-siltstone ratio in a given exposure typically ranges from ~5:1 to ~1:10. Sandstone-rich units are commonly broadly lenticular and thin to thick bedded, and in places they appear to occupy paleochannels. Sandstone beds are as thick as 10 m but mostly less than 2 m. Sandstone is mostly fine to medium grained, silty, feldspathic, and locally arkosic. On weathered surfaces sandstones display various shades of maroon, pale green, tan, and gray. Horizontal lamination and cross lamination, including trough cross lamination, are common. Sandstone is typically well indurated and forms resistant tabular, flaggy, or ledgy outcrops and, where steeply tilted, dip slopes and hogbacks. Small pebbly lenses are locally present in sandstone beds, and some thin (≤1 m thick) sandstone intervals, commonly near the base of beds, contain subrounded mudstone rip-up clasts.

Mudstone is typically silty to sandy and locally grades into siltstone and, rarely, fine-grained sandstone. Mudstone and siltstone are typically pale to dark maroon, reddish maroon, and brownish maroon, but in some places they are pale green or olive green. Mudstone is thin to very thin bedded and commonly laminated. Intervals of nearly pure mudstone range from less than 10 cm to at least 10 m thick. Some mudstone and siltstone bedding planes contain fossil mud cracks, ripple marks, worm burrows and (or) other trace fossils. Mudstone exhibits hackly to spheroidal fracturing on weathered surfaces. Most mudstone-rich intervals are poorly exposed and form gentle slopes.

Late Oligocene age of upper unit is based on Arikareean vertebrate fossils reported from the underlying middle unit 16–26 km west of map area (Weaver and Kleinpell, 1963; Howard, 1995) and on the Miocene-Oligocene boundary recognized at the base of the Rincon Shale (Tr) farther up section (David Bukry, oral commun., 1994).

Environment of deposition of Sespe upper sandstone and mudstone unit, which is equivalent to lithofacies D of Howard (1995), has been interpreted as progressing upward from braided to meandering river channels and interchannels (Howard, 1995). Unit previously mapped as part of the Sespe Formation (Upson, 1951; Lian, 1954; Dibblee, 1987a,b; Tan and Clahan, 2004; Tan and Jones, 2006). Upper unit decreases in thickness from about 920 m in the Casitas Valley area to about 700 m north of Lake Casitas. Upper Sespe unit is locally prone to landsliding, particularly on steeper slopes

Tspm **Middle conglomerate and sandstone unit (Oligocene)—**Conglomerate, sandstone, and mudstone interbedded in proportions that vary both laterally and down section; relative proportion of conglomerate increases towards base of unit, but conglomerate is strongly subordinate to sandstone and mudstone in some intervals. Conglomeratic depositional units range from laterally extensive to narrowly lenticular and thin to thick bedded (as thick as 15 m), and in some places they appear to occupy paleochannels. Conglomerate and conglomeratic sandstone typically contain subangular to well-rounded pebbles and cobbles supported in a medium- to coarse-grained sand and silty sand matrix. Clasts are polymict and include abundant chert (red, green, and black), greenstone, and lithic sandstone derived from Franciscan Complex terrane(s), arkosic sandstone derived from Coldwater Sandstone (Tcw), and quartzitic, metamorphic (including augen gneiss), and granitoid rocks derived from Mojave Desert terrane(s) (Howard, 1995). Sandstone is mostly medium to coarse grained, pebbly, silty, and feldspathic to lithic; rare sandstone beds are arkosic. On weathered surfaces, conglomerates and sandstones display various shades of maroon and, less commonly, tan and pale greenish gray. Horizontal lamination and cross lamination, including trough cross lamination, are common, particularly in sandstones. Rarely, sandstone beds exhibit evidence of soft-sediment deformation, and sediment-filled fossil burrows are apparent on some sandstone bedding planes. Commonly, conglomerates and sandstones are moderately indurated and resistant and form tabular, flaggy, or ledgy outcrops.

Mudstone is typically silty to sandy and locally grades into siltstone and, more rarely, fine-grained sandstone. Mudstone is thin to very thin bedded and commonly laminated. Ripple marks are common. Mudstone-rich intervals range in thickness from thin partings to 20 m, and in some intervals proportion of mudstone greatly exceeds that of sandstone and conglomerate. Mudstone is maroon, maroonish red, reddish brown, and, rarely, pale greenish gray and exhibits hackly to spheroidal fracturing on weathered surfaces. Most mudstone-rich intervals are poorly exposed and form gentle slopes.

Upper contact of middle unit mapped at stratigraphically highest conglomerate bed. A disconformity at base of middle unit generally expressed by abrupt change from maroonish sandstone and conglomerate of mixed provenance (middle unit) to pale pinkish-gray sandstone and conglomerate of largely granitic and metamorphic provenance (lower Sespe unit). Lowermost part of middle Sespe unit locally contains one or more beds of sandstone and (or) conglomerate that strongly resemble those characterizing the lower Sespe unit; lower contact of middle Sespe unit mapped at base of lowermost maroon, middle Sespe-like conglomerate or sandstone bed.

Middle conglomerate and sandstone unit is primarily equivalent to Sespe lithofacies C of Howard (1995). Oligocene age of middle unit based on Arikareean vertebrate fossils (*Sespia nitida* Leidy) reported from the unit above disconformity in foothills north of Santa Barbara 16–26 km west of map area (Weaver and Kleinpell, 1963; Howard, 1995).

Middle unit previously mapped as part of the Sespe Formation (Upson, 1951; Lian, 1954; Dibblee, 1987a,b; Tan and Clahan, 2004; Tan and Jones, 2006). Middle unit has a thickness of about 750 m west of Rincon Creek and in the Laguna Ridge area. Unit is moderately susceptible to landsliding particularly on steeper slopes along the lower flanks of the Santa Ynez Mountains and Laguna Ridge

Tspl **Lower conglomerate and sandstone unit (lower Oligocene? and upper Eocene)—** Conglomerate, conglomeratic sandstone, sandstone, mudstone, and minor shale interbedded in proportions that vary both laterally and vertically through the section. Conglomeratic depositional units range from laterally extensive to narrowly lenticular and medium to thick bedded, and at some places, appear to occupy paleochannels. Conglomerate and conglomeratic sandstone contain pebbles, cobbles, and rare boulders supported in a medium-grained to very coarse-grained, locally arkosic sandstone matrix. Clasts are polymict and include abundant subrounded to well-rounded quartzitic, granitoid, metamorphic, and volcanic clasts derived from Mojave Desert source terrane(s) (Howard, 1995). Sandstone is mostly medium to very coarse grained, pebbly, feldspathic, and locally arkosic. On weathered surfaces, conglomerates and sandstones mostly exhibit distinctive shades of salmon gray, reddish gray, pale-pinkish gray, and pale tan; reddish-brown iron-oxide staining is locally prevalent. Horizontal lamination and cross lamination, including trough cross lamination, are very common, particularly in sandstones. Conglomerates and sandstones are moderately to well indurated, resistant, and form flaggy, blocky, and ledgy outcrops and hogbacks.

Mudstone is typically silty to sandy and locally grades into siltstone and, more rarely, fine-grained sandstone. Intervals of fissile shale are locally present. Mudstone is thin to very thin bedded and commonly laminated. Mudstone-rich intervals range in thickness from thin partings to 5 m. Mudstone is maroon, maroonish red, gray, greenish-gray, and reddish brown and exhibits hackly to spheroidal fracturing on weathered surfaces. Most mudstone-rich intervals are poorly exposed and form gentle slopes.

Disconformable upper contact of lower conglomerate and sandstone unit is commonly expressed by 3- to 10-m-thick interval of conspicuous deep-reddish-brown, massive-to-bedded, silty to sandy claystone and mudstone; upper contact mapped at base of lowermost maroon, middle Sespe-like conglomerate or sandstone bed. Basal contact of lower unit, exposed in northwestern map area, generally marked by sharp change from pinkish- and reddish-gray, laminated sandstone and conglomerate (Sespe) to pale yellow-tan to buff, massive, locally oyster-shell-bearing sandstone of the underlying Coldwater Sandstone (Tcw). Locally lower contact is gradational, expressed by an interval of Coldwater-like sandstone containing Sespe-like maroon mudstone and siltstone interbeds; in such areas basal Sespe contact is mapped at top of uppermost Coldwater-like sandstone bed. The gradational nature of the basal contact is consistent with a late Eocene age for part or all of the lower conglomerate and sandstone unit.

The lower unit is primarily equivalent to Sespe lithofacies A of Howard (1995). Unit previously mapped as part of the Sespe Formation (Upson, 1951; Dibblee, 1987a,b; Tan and Clahan, 2004; Tan and Jones, 2006); as the lower member of the Sespe Formation (Lian, 1954); and as pink sandstone and red claystone of the Sespe Formation (Dibblee, 1987a). The lower conglomerate and sandstone unit is exposed along strike for several kilometers near the northwestern border of the map area, and the upper part also in a separate, small strip along the northeastern border just west of the Ventura River; in the northwestern exposures the unit decreases in thickness eastward from about 150 m west of Rincon Creek to less than 60 m near Laguna Ranch (about 1 km south of La Granada Mountain)

Tcw **Coldwater Sandstone (upper? and middle Eocene)—**Shallow-marine sandstone with subordinate interbeds and thin intervals of siltstone, shale, and mudstone. The unit is present near the northwest border of map area where it forms ridges, spurs, and steep dip slopes and hogbacks along the Santa Ynez Mountains front. Sandstone is mostly fine- to medium-grained, feldspathic and partly arkosic, locally silty to clayey or micaceous, and locally weakly cemented with calcium carbonate. Sandstone forms thin, tabular beds as well as medium to thick beds, some of which are massive and bioturbated whereas others contain planar, wavy, or cross laminations. Some sandstone beds contain rare, thin siltstone and shale partings. Sandstone is typically pale gray and greenish gray on fresh surfaces and weathers to distinctive, pale shades of buff, greenish-buff, yellowish-tan,

tan, and brown. Some beds and intervals as thick as 3 m, especially in the upper part of the unit, contain rare to conspicuously abundant oyster shells and shell fragments (*Ostrea idriaensis*, Weaver and Kleinpell, 1963), and numerous other fossil mollusks have been previously identified throughout the unit (for example, Weaver and Kleinpell, 1963). Other beds and intervals contain rare to common fossil wood fragments that in places contrast visually with the surrounding rock due to their dark-gray to reddish-brown color. Lenses and thin intervals of conglomeratic sandstone are locally present in the uppermost Coldwater near its contact with the overlying lower unit of the Sespe Formation (Tspl). Sandstone beds and sandstone-rich intervals typically crop out as resistant, blocky ledges and cliffs that form prominent hogbacks where steeply dipping.

Siltstone, shale, and mudstone form interbeds as thin as 1 cm and bedded intervals as thick as 5 m. These fine-grained rocks mostly exhibit pale to dark shades of gray, olive gray, greenish gray, and olive tan. Some siltstone beds are micaceous and contain fossil wood fragments. Siltstones and finer-grained rocks of the Coldwater are considerably less resistant and more poorly exposed than the sandstones. Some siltstone, shale, and mudstone intervals in uppermost part of unit are maroon, suggesting that contact with overlying nonmarine beds of the Sespe Formation is gradational. Upper Coldwater contact mapped at top of uppermost Coldwater-like sandstone bed.

Regionally, age of Coldwater has been determined to be late and (or) middle Eocene (Narizian) (Kleinpell and Weaver, 1963; Dibblee, 1966; Howard, 1995; Campion and others, 1996; Prothero, 2001) on basis of paleontologic, magnetostratigraphic, and sequence stratigraphic correlations. Unit previously mapped as Tejon Formation (Upson, 1951) and Coldwater Sandstone (Lian, 1954; Dibblee, 1987a; Tan and Clahan, 2004). Base of Coldwater is not exposed in map area; unit is about 750 to 1,000 m thick regionally (Dibblee, 1982)

Acknowledgments

The new mapping effort was funded by the USGS National Cooperative Geologic Mapping Program's BALANCE (BAsins and LANdscape Co-Evolution) and BIGFOOT (BIG-storm FOOTprint on California and future hazards) Projects. The support and encouragement of BALANCE project co-chiefs Jonathan Matti and Robert Powell and BIGFOOT project chief Kevin Schmidt allowed the mapping effort to continue smoothly to completion. I am grateful to Rick Stanley (USGS) for his expert stratigraphic and biostratigraphic advice and contributions both in the field and from afar. Kris McDougall and John Barron (both USGS) conducted key paleontologic and biostratigraphic analyses for several of the map units. Discussions in the field with Richard Heermance (California State University, Northridge) during early stages of the mapping effort were helpful in elucidating and interpreting the Quaternary map units. Numerous discussions with Larry Gurrola about the geology of the map area throughout the mapping project were invaluable. Private-land access kindly granted by landowners too numerous to list individually was critical to complete the mapping. Constructive reviews by Larry Gurrola, Dave Lidke, and Paco Van Sistine improved the quality of the map, map text, and digital map database. The late Tom Dibblee is acknowledged for his numerous pioneering and far-reaching contributions to our understanding of the geology of the region surrounding and including the map area, and of southern California in general.

References Cited

Arends, R.G., and Blake, G.H., 1986, Biostratigraphy and paleoecology of the Naples Bluff coastal section based on diatoms and benthic foraminifera, *in* Casey, R.E., and Barron, J.A., eds., Siliceous microfossil and microplankton studies of the Monterey Formation and modern analogs: Los Angeles, Society of Economic Paleontologists and Mineralogists, Pacific Section, Book 45, p. 121–135.

Arnold, Ralph, 1907, Geology and oil resources of the Summerland district, Santa Barbara County, California: U.S. Geological Survey Bulletin, no. 321, 93 p. [Also available at http://pubs.er.usgs.gov/publication/b321.]

Barron, J.A., 1986, Updated diatom biostratigraphy for the Monterey Formation of California, *in* Casey, R.E., and Barron, J.A., eds., Siliceous microfossil and microplankton studies of the Monterey Formation and modern analogs: Society of Economic Paleontologists and Mineralogists, Pacific Section, Book 45, p. 105–119.

Bezore, Stephen, and Wills, C.J., 2000, Landslide hazard maps of southeastern Santa Barbara County, California: California Division of Mines and Geology Open-File Report 99–12, 4 sheets, scale 1:24,000.

Blake, G.H., 1994, Detailed biostratigraphy and paleoenvironmental interpretation of the Naples Bluff section, *in* Hornafius, J.S., ed., Field guide to the Monterey Formation between Santa Barbara and Gaviota, California: Bakersfield, Calif., Pacific Section, American Association of Petroleum Geologists, p. 17–28.

Campion, K.M., Sullivan, M.D., May, J.A., and Warme, J.E., 1996, Sequence stratigraphy along a tectonically active margin, Paleogene of southern California, *in* Abbott, P.L., and Cooper, J.D., eds., Field Conference Guide 1996: American Association of Petroleum Geologists, Pacific Section, GB 73, and Society for Sedimentary Geology (SEPM), Pacific Section, Book 80, p. 125–187.

Clark, M.N., 1982, Tectonic geomorphology and neotectonics of the Ojai Valley and upper Ventura River: Santa Barbara, University of California Santa Barbara, M.S. thesis, 77 p., 5 pls.

Cohen, K.M., Finney, S.C., Gibbard, P.L. and Fan, J.X., 2013, The ICS International Chronostratigraphic Chart: Episodes, v. 36, no. 3, p. 199–204.

Cruden, D.M., and Varnes, D.J., 1996, Landslide types and processes, *in* Turner, A.K., and Schuster, R.L., eds., Landslides—Investigation and mitigation: Washington, D.C., National Academy Press, p. 36–75.

DePaolo, D.J., and Finger, K.L., 1991, High resolution strontium isotope stratigraphy and biostratigraphy of the Miocene Monterey Formation, central California: Geological Society of America Bulletin, v. 103, no. 1, p. 112–124.

DeVecchio, D.E., Heermance, R.V., Fuchs, Markus, and Owen, L.A., 2012, Climate-controlled landscape evolution in the western Transverse Ranges, California—Insights from Quaternary geochronology of the Saugus Formation and strath terrace flights: Lithosphere, v. 4, no. 2, p. 110–130.

Dibblee, T.W., Jr., 1966, Geology of the central Santa Ynez Mountains, Santa Barbara County, California: California Division of Mines and Geology Bulletin 186, 99 p.

Dibblee, T.W., Jr., 1982, Geology of the Santa Ynez-Topatopa Mountains, Southern California, *in* Fife, D.L., and Minch, J.A., eds., Geology and mineral wealth of the California Transverse Ranges: Santa Ana, California, South Coast Geological Society Annual Symposium and Guidebook no. 10, p. 41–56.

Dibblee, T.W., Jr., 1987a, Geologic map of the White Ledge Peak quadrangle, Santa Barbara and Ventura Counties, California: Santa Barbara Museum of Natural History, Dibblee Geological Foundation Map DF–11, scale 1:24,000.

Dibblee, T.W., Jr., 1987b, Geologic map of the Matilija quadrangle, Ventura County, California: Santa Barbara Museum of Natural History, Dibblee Geological Foundation Map DF–12, scale 1:24,000.

Dibblee, T.W., Jr., 1988, Geologic map of the Ventura and Pitas Point quadrangles, Ventura County, California: Santa Barbara Museum of Natural History, Dibblee Geological Foundation Map DF–21, scale 1:24,000.

Dickinson, W.R., 1995, Paleogene depositional systems of the western Transverse Ranges and adjacent southernmost Coast Ranges, California, *in* Fritsche, A.E., ed., Cenozoic Paleogeography of the western United States II: Santa Fe Springs, Calif., Pacific Section SEPM (Society for Sedimentary Geology), p. 53–83.

Doblas, Miguel, 1998, Slickenside kinematic indicators: Tectonophysics, v. 295, p. 187–197.

Garrison, R.E., and Ramirez, P.C., 1989, Conglomerates and breccias in the Monterey Formation and related units as reflections of basin margin history, *in* Colburn, I.P., Abbott, P.L., and Minch, John, eds., Conglomerates in basin analysis—A symposium dedicated to A.O. Woodford: Bakersfield, Calif., Pacific Section, Society of Economic Paleontologists and Mineralogists, Book 62, p. 189–206.

Gurrola, L.D., Selting, A.J., Keller, E.A., Tierney, T.E., Hartleb, R.D., Trecker, M.A., and Dibblee, T.W., Jr., 2001, Neotectonics of the Santa Barbara fold belt, California, *with a section on* Investigation of the Mission debris flow deposit, Santa Barbara, California, by Selting, A.J. and Urban, R.J., *in* Dunne, G., and Cooper, J., compilers, Geologic excursions in southwestern California: Pacific Section, Society of Economic Paleontologists and Mineralogists, Book 89, p. 21–100.

Gurrola, L.D., Keller, E.A., Chen, J.H., Owen, L.A., and Spencer, J.Q., 2014, Tectonic geomorphology of marine terraces—Santa Barbara fold belt, California: Geological Society of America Bulletin, v. 126, n.1/2, p. 219–233.

Gurrola, L.D., DeVecchio, D.E., and Keller, E.A., 2010, Rincon Mountain megaslide—La Conchita, Ventura County, California: Geomorphology, v. 114, p. 311–318, doi:10.1016/j.geomorph.2009.07.013.

Hornafius, J.S., 1994a, Field trip road log to the Monterey Formation between Santa Barbara and Gaviota, California, *in* Hornafius, J.S., ed., Field guide to the Monterey Formation between Santa Barbara and Gaviota, California: Bakersfield, Calif., Pacific Section, American Association of Petroleum Geologists, p. 107–123.

Hornafius, J.S., 1994b, Overview of the stratigraphy of the Monterey Formation along the coastline between Santa Barbara and Gaviota, California, *in* Hornafius, J.S., ed., Field guide to the Monterey Formation between Santa Barbara and Gaviota, California: Bakersfield, Calif., Pacific Section, American Association of Petroleum Geologists, p. 1–15.

Hornafius, J.S., Luyendyk, B.P., Terres, R.R., and Kamerling, M.J., 1986, Timing and extent of Neogene tectonic rotation in the western Transverse Ranges, California: Geological Society of America Bulletin, v. 97, p. 1476–1487.

Howard, J.L., 1995, Conglomerates of the upper middle Eocene to lower Miocene Sespe Formation along the Santa Ynez Fault—Implications for the geologic history of the eastern Santa Maria basin area, chapter H *of* Keller, M.A., ed., Evolution of Sedimentary Basins/Onshore Oil and Gas Investigations—Santa Maria Province, U.S. Geological Survey Bulletin 1995–H,I, p. H1–H37. [Also available at http://pubs.er.usgs.gov/publication/b1995HI.]

Huftile, G.J., and Yeats, R.S., 1995, Convergence rates across a displacement transfer zone in the western Transverse Ranges, Ventura basin, California: Journal of Geophysical Research, v. 100, no. B2, p. 2043–2067.

Ingle, J.C., Jr., 1980, Cenozoic paleobathymetry and depositional history of selected sequences within the southern California continental borderland, *in* Sliter, W.V., ed., Studies in marine micropaleontology and paleoecology—A memorial volume to Orville L. Bandy: Cushman Foundation for Foraminiferal Research, Special Publication No. 19, p. 163–195.

Izett, G.A., Naeser, C.W., and Obradovich, J.D., 1974, Fission-track age of zircons from an ash bed in the Pico Formation (Pliocene and Pleistocene) near Ventura, California [abs.]: Geological Society of America, Annual Meeting, Cordilleran Section, Program with Abstracts, p. 197.

Jackson, P.J., and Yeats, R.S., 1982, Structural evolution of Carpinteria basin, western Transverse Ranges, California: American Association of Petroleum Geologists Bulletin, v. 66, p. 805–829.

Kear, J., 2005, Hydrogeology of the Ojai Groundwater Basin—Storativity and confinement, Ventura County, California: Northridge, California State University, M.S. thesis, 179 p.

Kleinpell, R.M., 1938, Miocene stratigraphy of California: Tulsa, Okla., American Association of Petroleum Geologists, 450 p.

Kleinpell, R.M., 1980, History of stratigraphic paleontology of west coast Tertiary, *in* Kleinpell, R.M., The Miocene stratigraphy of California revisited: Tulsa, Okla., American Association of Petroleum Geologists, Studies in Geology no. 11, p. 4–53.

Kleinpell, R.M., and Weaver, D.W., 1963, Oligocene biostratigraphy of the Santa Barbara embayment, California: University of California Publications in Geological Sciences, v. 43, 250 p.

Lajoie, K.R., Kern, J.P., Wehmiller, J.F., Kennedy, G.L., Mathieson, S.A., Sarna-Wojcicki, A.M., Yerkes, R.F. and McCrory, P.A., 1979, Quaternary marine shorelines and crustal deformation, San Diego to Santa Barbara, California, *in* Abbott, P.L., ed., Geological excursions in the southern California area, Guidebook for field trips, Geological Society of America Annual Meeting, Nov. 1979: San Diego, Calif., Department of Geological Sciences, San Diego State University, p. 3–15.

Lian, H.M., 1954, Geology of the Carpinteria district, Santa Barbara County, *in* Jahns, R.H., ed., Geology of southern California: California Division of Mines and Geology Bulletin 170, map sheet 25.

Luyendyk, B.P., 1991, A model for Neogene crustal rotations, transtension, and transpression in southern California: Geological Society of America Bulletin, v. 103, no.11, p. 1528–1536.

McKay, H.L., 2011, Quaternary stratigraphy and geologic evolution of Ojai and Upper Ojai Valleys, Western Transverse Ranges, California: Northridge, California State University, M.S. thesis, 48 p.

Minor, S.A., Kellogg, K.S., Stanley, R.G., Gurrola, L.D., Keller, E.A., and Brandt, T.R., 2009, Geologic map of the Santa Barbara coastal plain area, Santa Barbara County, California: U.S. Geological Survey Scientific Investigations Map 3001, scale 1:25,000, 1 sheet, pamphlet, 38 p. [Also available at http://pubs.usgs.gov/sim/3001/.]

Muhs, D.R., Rockwell, T.K., and Kennedy, G.L., 1992, Late Quaternary uplift rates of marine terraces on the Pacific coasts of North America, southern Oregon to Baja California Sur: Quaternary International, v. 15–16, p. 121–133.

Muir, K.S., 1968, Ground-water reconnaissance of the Santa Barbara-Montecito area, Santa Barbara County, California: U.S. Geological Survey Water-Supply Paper 1859–A, 28 p. [Also available at http://pubs.er.usgs.gov/publication/wsp1859A.]

Namson, J.S., and Davis, T.L., 1988, Structural transect of the western Transverse Ranges, California: Implications for lithospheric kinematics and seismic risk evaluation: Geology, v. 16, p. 675–679.

Patterson, R.T., Brunner, C.A., Capo, Rosemary, and Dahl, Jeremy, 1990, A paleoenvironmental study of early to middle Pleistocene foraminifera of the Santa Barbara Formation at Santa Barbara, California: Journal of Paleontology, v. 64, no. 1, p. 1–25.

Petit, J.P., 1987, Criteria for the sense of movement on fault surfaces in brittle rocks: Journal of Structural Geology, v. 9, no. 5/6, p. 597–608.

Prothero, D.R., 2001, Magnetostratigraphic tests of sequence stratigraphic correlations from the Southern California Paleogene: Journal of Sedimentary Research, v. 71, no. 4, p. 526–536.

Rigsby, C.A., 1998, Paleogeography of the Western Transverse Range Province, California—New evidence for the late Oligocene and early Miocene Vaqueros Formation, chapter T *of* Keller, M.A., ed., Evolution of Sedimentary Basins/Offshore Oil and Gas Investigations—Santa Maria Province: U.S. Geological Survey Bulletin 1995–T,U,V, p. T1–T18. [Also available at http://pubs.er.usgs.gov/publication/b1995TUV.]

Rockwell, T.K., 1983, Soil chronology, geology and neotectonics of the northern central Ventura Basin: Santa Barbara, University of California Santa Barbara, Ph.D. dissertation, 425 p.

Rockwell, T.K., Keller, E.A., Clark, M.N., and Johnson, D.L., 1984, Chronology and rates of faulting of Ventura River terraces, California: Geological Society of America Bulletin, v. 95, p. 1466–1474.

Rockwell, T.K., 1988, Neotectonics of the San Cayetano fault, Transverse Ranges, California: Geological Society of America Bulletin, v. 100, p. 500–513.

Rockwell, T.K., Nolan, Jeff, Johnson, D.L., and Patterson, R.H., 1992, Ages and deformation of marine terraces between Point Conception and Gaviota, western Transverse Ranges, California, *in* Fletcher, C.H. and Wehmiller, J.F., eds., Quaternary coasts of the United States—Marine and Lacustrine systems: Society of Economic Paleontologists and Mineralogists Special Publication 48, p. 333–341.

Stanley, R.G., Cotton, M.L., Bukry, David, Filewicz, M.V., Valin, Z.C., and Vork, D.R., 1994, Stratigraphic revelations regarding the Rincon Shale (lower Miocene) in the Santa Barbara coastal area, California [abs.]: American Association of Petroleum Geologists Bulletin, v. 78, no. 4, p. 675–676.

Stanley, R.G., Valin, Z.C., and Pawlewicz, M.J., 1992, Rock-Eval pyrolysis and vitrinite reflectance results from outcrop samples of the Rincon Shale (lower Miocene) collected at the Tajiguas Landfill, Santa Barbara County, California: U.S. Geological Survey Open-File Report 92–571, 27 p. [Also available at http://pubs.er.usgs.gov/publication/ofr92571.]

Tan, S.S., and Clahan, K.B., 2004, Geologic map of the White Ledge Peak 7.5′ quadrangle, Santa Barbara and Ventura Counties, California—A digital database: California Geological Survey Preliminary Geologic Map, scale 1:24,000. [Also available at ftp://ftp.consrv.ca.gov/pub/dmg/rgmp/Prelim_geo_pdf/White_Ledge_Pk_prelim.pdf.]

Tan, S.S., and Jones, T.A., 2006, Geologic map of the Matilija 7.5’ quadrangle, Ventura County, California—A digital database: California Geological Survey Preliminary Geologic Map, scale 1:24,000. [Also available at ftp://ftp.consrv.ca.gov/pub/dmg/rgmp/Prelim_geo_pdf/Matilija_prelim.pdf.]

Tennyson, M.E., and Isaacs, C.M., 2001, Geologic setting and petroleum geology of the Santa Maria and Santa Barbara basins, coastal California, *in* Isaacs, C.M., and Rullkötter, Jürgen, eds., The Monterey Formation—From rocks to molecules: Columbia University Press, New York, p. 206–229.

U.S. Geological Survey Geologic Names Committee, 2010, Divisions of geologic time–major chronostratigraphic and geochronologic units: U.S. Geological Survey Fact Sheet 2010–3059, 2 p. [Also available at http://pubs.usgs.gov/fs/2010/3059/.]

Upson, J.E., 1951, Geology and ground-water resources of the south-coast basins of Santa Barbara County, California: U.S. Geological Survey Water-Supply Paper 1108, 144 p. [Also available at http://pubs.er.usgs.gov/publication/wsp1108.]

Weaver, D.W., and Kleinpell, R.M., 1963, Oligocene biostratigraphy of the Santa Barbara embayment, California, Part II, Mollusks from the *Turritella variata* zone: University of California Publications in the Geological Sciences, v. 43, p. 81–118.

Wehmiller, J.F., Lajoie, K.R., Sarna-Wojcicki, A.M., Yerkes, R.F., Kennedy, G.L., Stephens, T.A., and Kohl, R.F., 1978, Amino-acid racemization dating of Quaternary mollusks, Pacific Coast, United States, *in* Zartman, R.E., ed., Short papers of the fourth international conference, geochronology, cosmochronolgy, isotope geology: U.S. Geological Survey Open-File Report 78–701, p. 445–448. [Also available at http://pubs.er.usgs.gov/publication/ofr78701.]

Wehmiller, J.F., 1992, Aminostratigraphy of southern California Quaternary marine terraces, *in* Fletcher, C.H., and Wehmiller, J.F., eds., Quaternary coasts of the United States—Marine and lacustrine systems: Society for Sedimentary Geology (SEPM) Special Publication 48, p. 317–321.

Williams, Howell, Turner, F.J., and Gilbert, C.M., 1982, Petrography—An introduction to the study of rocks in thin sections (2d ed.): San Francisco, W.H. Freeman and Company, 626 p.

Yeats, R.S., Lee, W.H.K., and Yerkes, R.F., 1987, Geology and seismicity of the eastern Red Mountain fault, Ventura County, *in* Morton, D.M., and Yerkes, R.F., eds., Recent reverse faulting in the Transverse Ranges, California: U.S. Geological Survey Professional Paper 1339, p. 161–167. [Also available at http://pubs.er.usgs.gov/publication/pp1339.]

Yerkes, R.F., Greene, H.G., Tinsley, J.C., and Lajoie, K.R., 1981, Maps showing seismotectonic setting of the Santa Barbara channel area, California: U.S. Geological Survey Miscellaneous Field Studies Map MF–1169, scale 1:250,000, 25 p. pamphlet. [Also available at http://pubs.er.usgs.gov/publication/mf1169.]

Yerkes, R.F., and Lee, W.H.K., 1987, Late Quaternary deformation in the western Transverse Ranges, *in* Morton, D.M., and Yerkes, R.F., eds., Recent reverse faulting in the Transverse Ranges, California: U.S. Geological Survey Professional Paper 1339, p. 71–82. [Also available at http://pubs.er.usgs.gov/publication/pp1339.]

Yerkes, R.F., Sarna-Wojcicki, A.M., and Lajoie, K.R., 1987, Geology and Quaternary deformation of the Ventura area, *in* Morton, D.M., and Yerkes, R.F., eds., Recent reverse faulting in the Transverse Ranges, California: U.S. Geological Survey Professional Paper 1339, p. 169–178. [Also available at http://pubs.er.usgs.gov/publication/pp1339.]

Publishing support provided by:
Denver Publishing Service Center, Denver, Colorado

For more information concerning this publication, contact:

Center Director, USGS Central Energy Resources Science Center
Box 25046, Mail Stop 939
Denver, CO 80225
(303) 236-1647

Or visit the Central Energy Resources Science Center Web site at:
http://energy.usgs.gov/

This publication is available online at:
http://dx.doi.org/10.3133/sim3321

Minor, S.A., and Brandt, T.R.—**Geologic Map of the Southern White Ledge Peak and Matilija Quadrangles, California**—Scientific Investigations Map 3321

ISSN 2329-132X (online)
http://dx.doi.org/10.3133/sim3321